The Abdus Salam
International Centre for Theoretical Physics

United Nations
Educational, Scientific and
Cultural Organization

IAEA
International Atomic Energy Agency

SMR/1848-T15

Course on Natural Circulation Phenomena and Modelling in Water-Cooled Nuclear Reactors

25 - 29 June 2007

T15 - Experimental Validation and Data Base of Simple Loop Facilities

P.K. Vijayan
Bhabha Atomic Research Centre (BARC), Mumbai, India

Strada Costiera 11, 34014 Trieste, Italy - Tel. +39 040 2240 111; Fax +39 040 224 163 - sci_info@ictp.it, www.ictp.it

EXPERIMENTAL VALIDATION AND DATABASE OF SIMPLE LOOP FACILITIES

P.K. Vijayan
Reactor Engineering Division,
Bhabha Atomic Research Centre, Mumbai, India

IAEA Course on Natural Circulation in Water-Cooled Nuclear Power Plants, ICTP, Trieste, Italy, 25-29 June, 2007 (Lecture : T-15)

OUTLINE OF THE LECTURE T#15

- INTRODUCTION
- STEADY STATE BEHAVIOUR OF 1-ϕ LOOPS
- STEADY STATE BEHAVIOUR OF 2-ϕ LOOPS
- STABILITY BEHAVIOUR OF 1-ϕ LOOPS
- EXPERIMENTAL DATABASE FOR INSTABILITY OF 2-ϕ LOOPS
- STATIC INSTABILITY OF 2-ϕ LOOPS
- DYNAMIC INSTABILITY OF 2-ϕ LOOPS
- CONCLUDING REMARKS

INTRODUCTION

Advantages of Simple loop Facilities

- Easy to construct and operate
- Minimum of instrumentation
- Phenomena taking place is easily traceable
- Large amount of easily reproducible data can be generated economically in a short time
- Theoretical and numerical modelling is far more easier
- Data interpretation is easy

INTRODUCTION – Contd.

Contribution of simple loop facilities

- Phenomenological understanding of NC process

. Hysteresis or conditional stability phenomenon,
. Nature of the unstable flow
- oscillatory modes, phase shift and flow regimes
. Flow redistribution in parallel channels

- Development of theoretical model and computer codes

- Steady state, transient and stability performance of NCS

- Development and testing of scaling laws

Topic of this lecture - **Contribution of simple loop facilities on the study of steady state and stability behaviour of single-phase and two-phase loops**

Steady state performance of single-phase loops

For an incompressible Boussinesq fluid

$$g\rho_0\beta\oint Tdz = \frac{RW^2}{2\rho}$$

Integrating and rearranging

$$W = \left[\frac{2\rho_0^2\beta g Q_h H}{RCp}\right]^{\frac{1}{3}} \quad or\ W \propto (Q_h)^{\frac{1}{3}}$$

The core or heater ΔT_h can be obtained as

$$\Delta T_h = \left[\frac{RQ_h^2}{2\rho_0^2\beta g H Cp^2}\right]^{\frac{1}{3}} or\ \Delta T_h \propto (Q_h)^{\frac{2}{3}}$$

For other orientations of source and sink

$$W = \left[\frac{2\rho_0^2\beta g Q_h \Delta Z_c}{RCp}\right]^{\frac{1}{3}}$$

Where ΔZ_c : C-L elev. diff. betn. sink and source

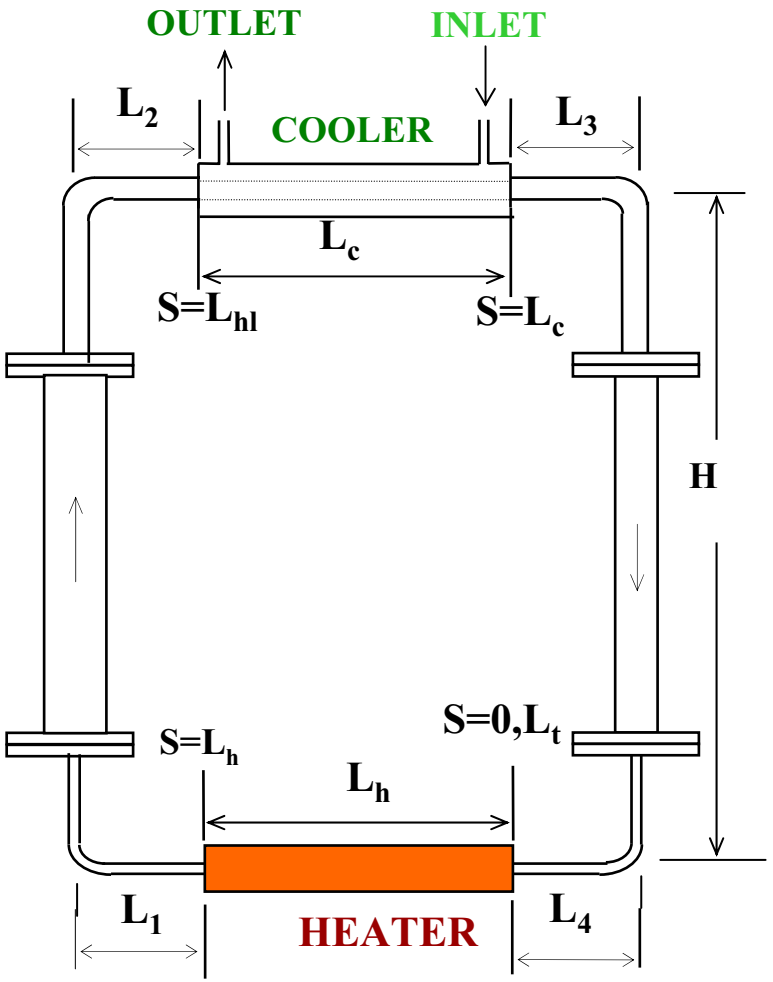

NC in a simple NDL

Generalized Flow Correlation

The total loop hydraulic resistance

$$R = \sum_{i=1}^{N} \left(\frac{fL}{D} + K \right)_i \frac{1}{A_i^2}$$

Replace the local loss coefficients K_i with an equivalent length, Le_i

$$Le_i = \frac{K_i D_i}{f_i} \quad \text{So that} \quad \left(L_{eff} \right)_i = L_i + Le_i$$

Define reference area and diameter for the NDL as

$$A_r = \frac{1}{L_t} \sum_{i=1}^{N} A_i L_i = \frac{V_t}{L_t} \quad and \quad D_r = \frac{1}{L_t} \sum_{i=1}^{N} D_i L_i$$

If the entire loop follows a friction law of the form $f_i = \dfrac{p}{\mathrm{Re}_i^b}$ then

$$\mathrm{Re} = C \left(\frac{Gr_m}{N_G} \right)^r \quad where \; N_G = \frac{L_t}{D_r} \sum_{i=1}^{N} \left(\frac{l_{eff}}{d^{1+b} a^{2-b}} \right)_i ; C = \left(\frac{2}{p} \right)^r \quad and \; r = \left(\frac{1}{3-b} \right)$$

Generalized Flow Correlation – Contd.

A Generalized correlation valid for all orientations can be obtained as before if linear variation of temperature is assumed in the cooler

$$\mathrm{Re} = C\left[\frac{(Gr_m)_{\Delta z_c}}{N_G}\right]^r$$

The error, E, introduced by this assumption is < 1% if $St_m < 1$

$$\mathrm{Re} = 0.1768\left[\frac{(Gr_m)_{\Delta z_c}}{N_G}\right]^{0.5}$$ fully laminar loop

$$\mathrm{Re} = 1.96\left[\frac{(Gr_m)_{\Delta z_c}}{N_G}\right]^{\frac{1}{2.75}}$$ fully turbulent loop

$$\mathrm{Re} = 0.3548\left[\frac{(Gr_m)_{\Delta z_c}}{N_G}\right]^{0.43}$$ transition region (empirical)

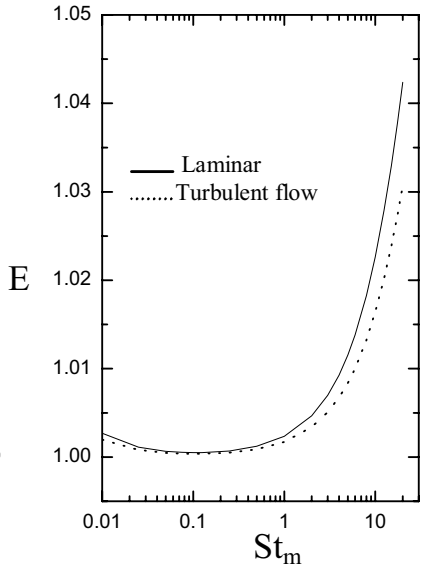

HHVC

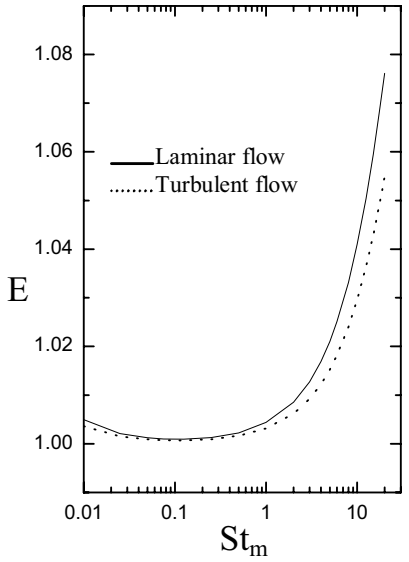

VHVC

Steady state performance of single-phase loops

The Generalized flow correlations were found useful to compare the performance of various loops

Uniform diameter loops (UDLs)
Nonuniform diameter loops (NDLs)

Database for UDLs

Total Number of loops : 14
Loop diameter : 6 to 40 mm
Loop height : 0.38 to 2.3 m
Total circulation length : 1.2 to 7.2 m
L_t/D ratio : 75 to 1100
Fluid used : mostly water and freon in one case
Pressure : near atmospheric to near critical pressure (freon)
Source and sink orientations: all four (HHHC, HHVC,VHHC and VHVC)
Loop types : Open and closed loops
Loop shapes : Rectangular, toroidal, figure-of-eight loops

Steady state performance of UDLs

Comparison of UDL data - Without local losses, $N_G=L_t/D$

- With local losses, $N_G=(L_{eff})_t/D$

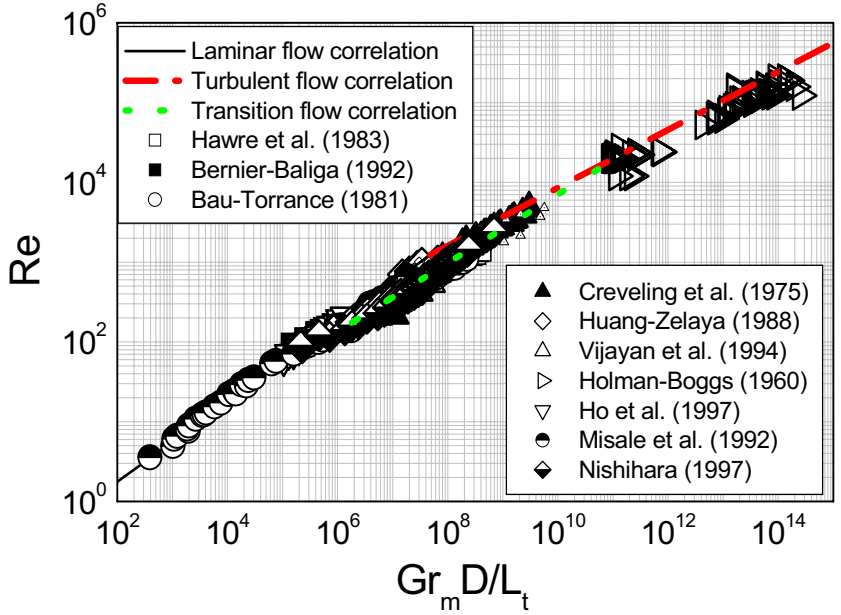

Without local losses

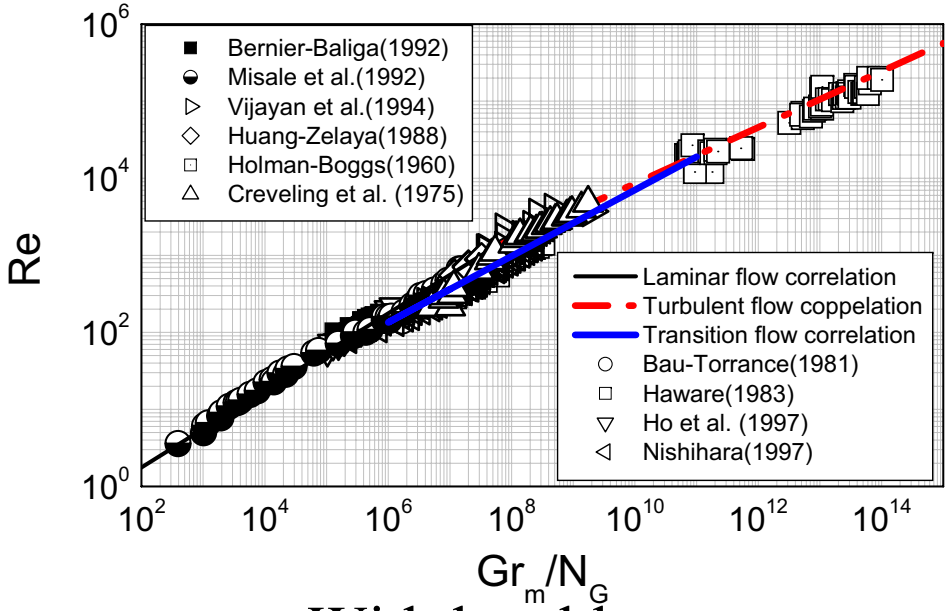

With local losses

Local losses are significant in the high Reynolds number zone

Good agreement with laminar flow correlation in the low Re zone and good agreement in the turbulent flow correlation in the high Re zone.

Steady state performance of NDLs

Most practical applications of NC employ NDLs

NDL database

Total Number of loops : 10
Loop diameter : 3.6 to 97 mm
Loop height : 1 to 26 m
Total circulation length : 10 to 125 m
Fluid used : water
Pressure : up to 90 bar
Source and sink orientations: HHVC and VHVC
Loop types : closed loops

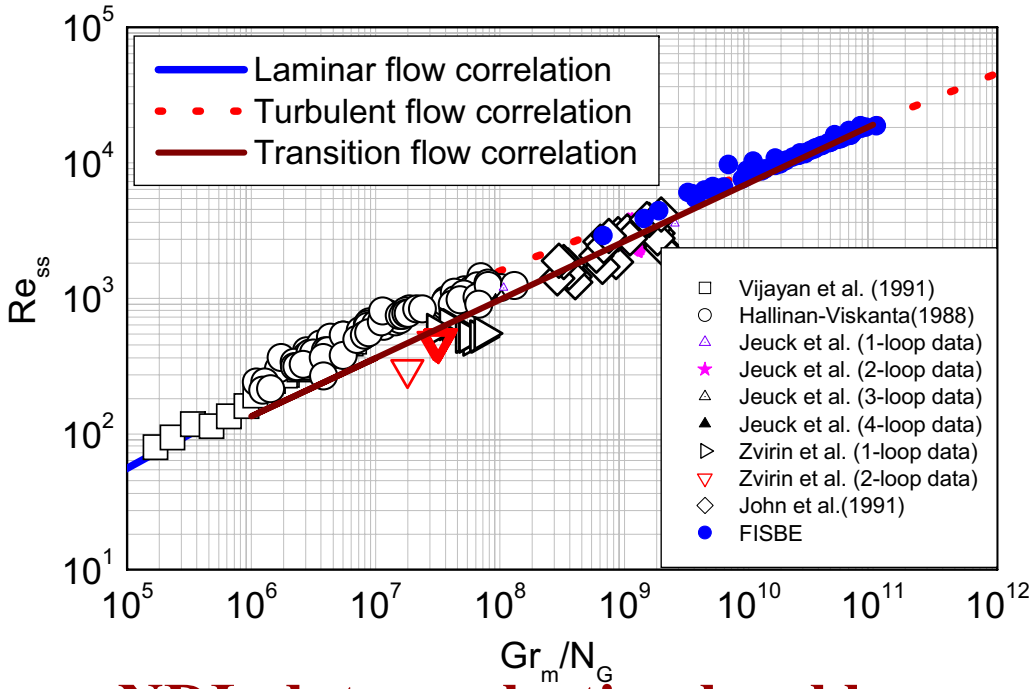

NDL data neglecting local losses

Loop shapes : Rectangular and figure-of-eight loops

Data for low Re agrees with laminar flow correlation and high Re data agrees with turbulent flow correlation

Steady state performance of Single-phase Loops

General Remarks

Laminar flow correlation is good for $Gr_m/N_G < 10^6$

Turbulent flow correlation is good for $Gr_m/N_G > 10^{10}$

Significant data scatter exists in $10^6 < Gr_m/N_G < 10^{10}$ as the loop is neither fully laminar nor fully turbulent. The empirical correlation is good in this region

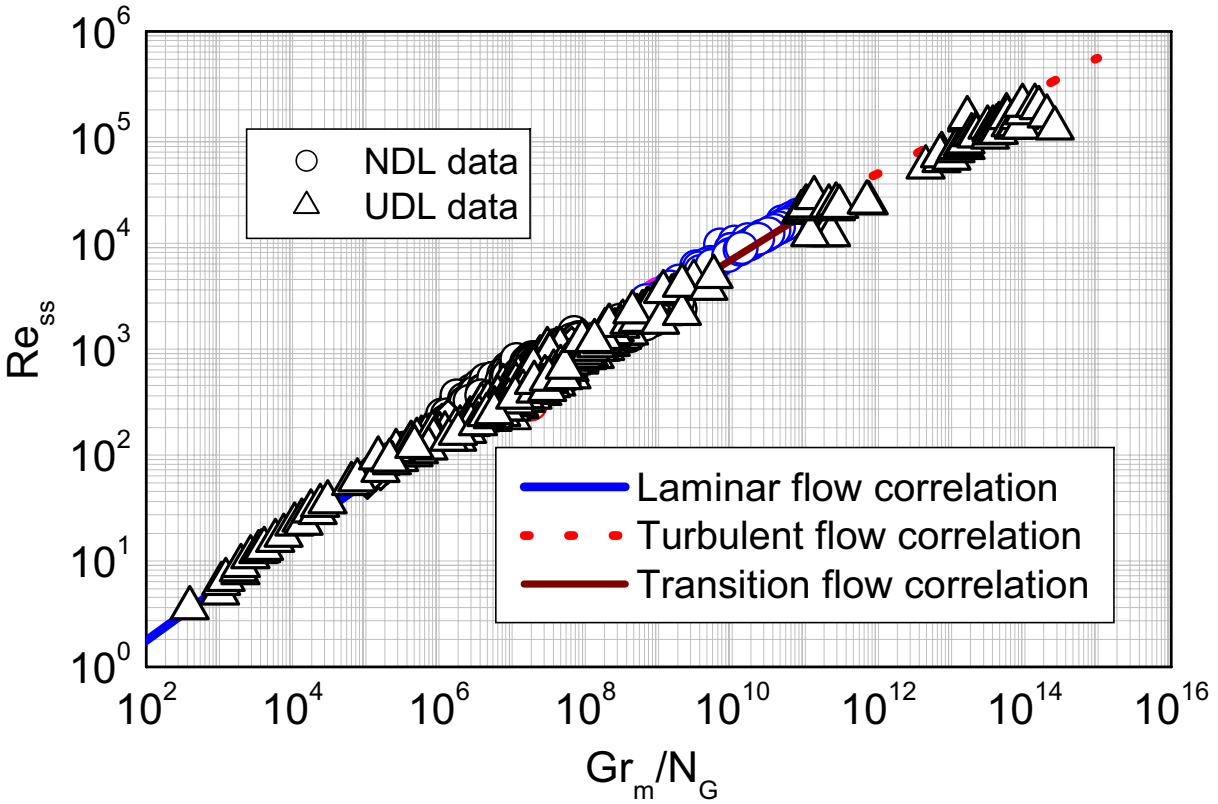

UDL and NDL data neglecting local losses

For specific loops good agreement with laminar flow correlation is obtained even up to Re of 1200 ($Gr_m/N_G < 5x10^7$). Similarly turbulent flow correlation is found to give good results for Re > 2000 ($Gr_m/N_G > 2x10^8$)

Steady State Performance (1-ϕ NC)

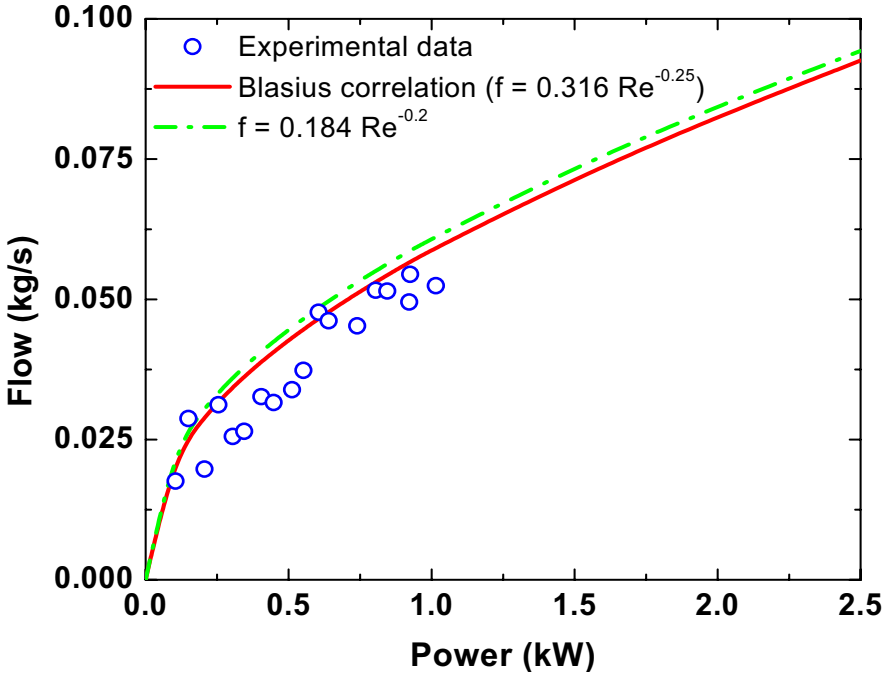

Measured and predicted flow rate for 26.9 mm i.d. loop

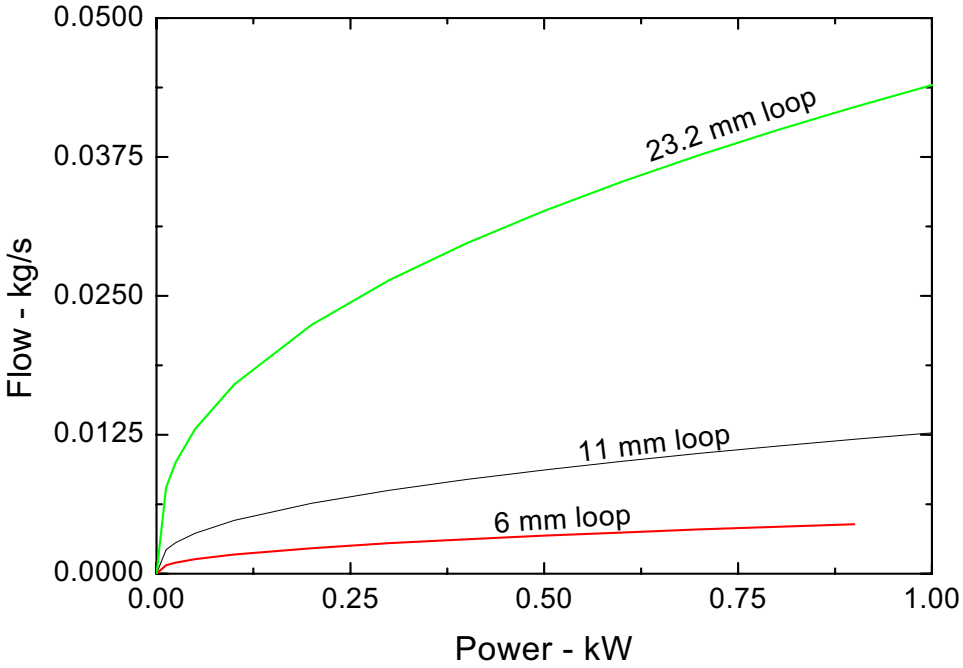

Effect of loop diameter on predicted flow rate

The flow rate increases with power as well as with loop diameter as expected.

Steady state Performance of Two-phase Loops

Based on the Homogeneous Equilibrium Model (HEM). The pressure losses in the system are negligible compared to the static pressure so that (constant pressure system) the fluid property variation with pressure is negligible.

The inlet subcooling is negligible so that the density variation in the single-phase heated section can be neglected.

Complete separation of steam and water is assumed to occur in the SD so that there is no liquid carryover with the steam and no vapor carry-under with water (see Figure)

A constant level is maintained in the SD, so that the single-phase lines always run full

The heater is supplied with a uniform heat flux and the SD can be approximated to a point heat sink. Heat losses are negligible

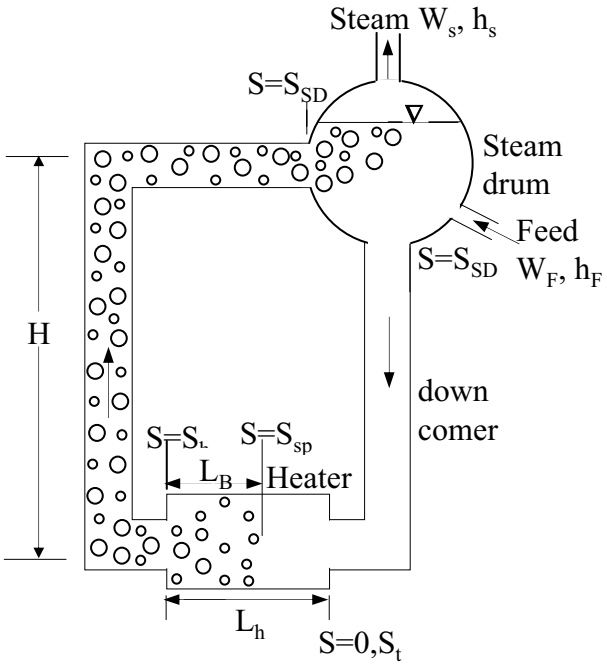

Loop relevant to BWRs

Steady state Performance of Two-phase Loops

The steady state one-dimensional governing equations for the two-phase NCS

$$\frac{dW}{ds}=0$$ **Conservation of mass**

$$\frac{W}{A_i}\frac{dh}{ds}=\begin{cases}\dfrac{4q_h''}{D_h} & heater\\ 0 & pipes\end{cases}$$ **Conservation of energy**

$$\frac{W^2}{A_i^2}\frac{d\mathrm{v}}{ds}=-\frac{dP}{ds}-\rho g\sin\theta-\frac{fW^2}{2D_i\rho A_i^2}-\frac{KW^2}{2\rho A_i^2 L_t}$$ **Conservation of momentum**

Integrating the momentum equation around the closed loop and noting that $\oint d\mathrm{v}=\oint dP=0$ we get

$$-g\oint\rho\,dz=\frac{W^2}{2\rho}\sum_{i=1}^{N_t}\left(\frac{fL}{DA^2}+\frac{K}{A^2}\right)_i=\frac{RW^2}{2\rho}$$ where dz=ds.sinθ

Steady state Performance of Two-phase Loops

Two-phase density in the buoyancy force term can be approximated as

$$\rho = \rho_r\left[1-\beta_h\left(h-h_l\right)\right]$$

where $$\beta_h = \left(\frac{1}{\mathrm{v}}\right)\left(\frac{\partial \mathrm{v}}{\partial \mathrm{h}}\right)_p$$

$$\rho = \alpha\rho_g + \left(1-\alpha\right)\rho_l$$

$$where\ \alpha = \frac{1}{1+\frac{1-x}{x}\frac{\rho_g}{\rho_l}}$$

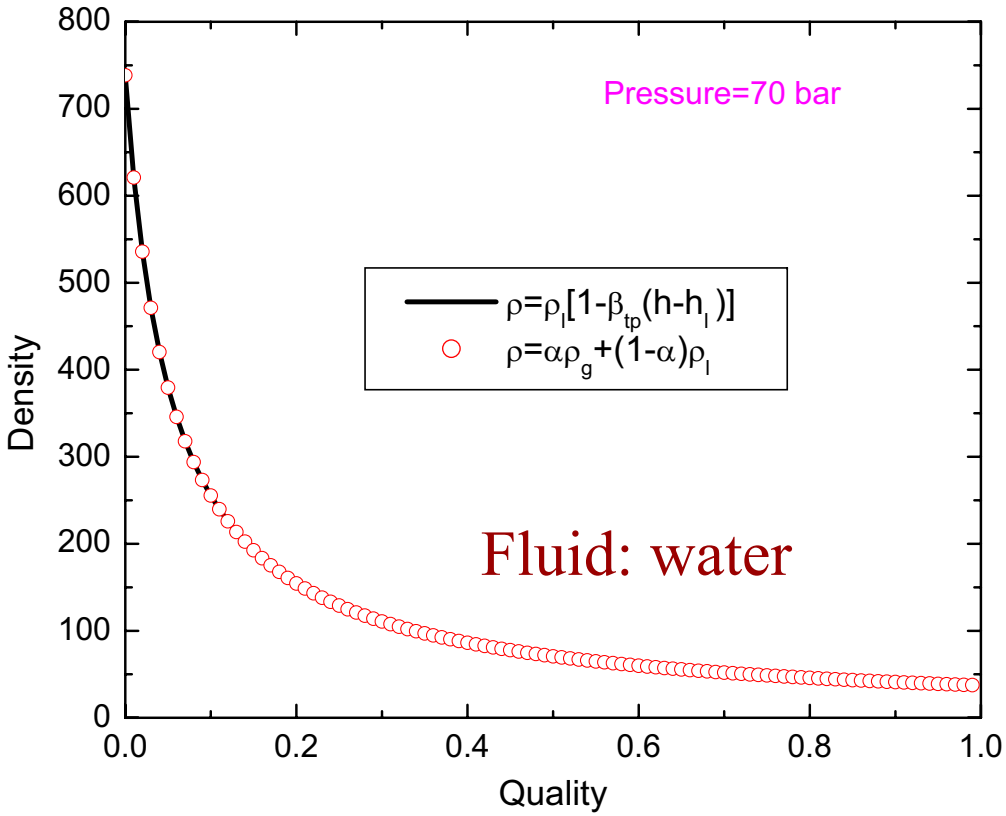

Density variation in the two-phase region

Both the definitions are equivalent for a constant pressure system in the two-phase regime if HEM is applicable

Steady state Performance of Two-phase Loops

If we can approximate β_h to be a constant over the loop, then

$$-g\rho_r \overline{\beta}_h \oint h\,dz = \frac{RW^2}{2\rho}$$

Noting that $\Delta h_{ss}=Q_h/W$, $W = \left[\frac{2\rho_r^2 \overline{\beta}_h g Q_h H}{R}\right]^{\frac{1}{3}}$

$$where\ R = \sum_{i=1}^{N_s}\left(\frac{fL}{DA^2}+\frac{K_{sp}}{A^2}\right)_i + \sum_{i=N_s+1}^{N_B}\left(\frac{\overline{\phi}_{LO}^2 fL}{DA^2}+\frac{K_{tp}}{A^2}\right)_i + \phi_{LO}^2 \sum_{i=N_B+1}^{N_{tp}}\left(\frac{fL}{DA^2}+\frac{K_{tp}}{A^2}\right)_i$$

Replacing the local loss coefficients in terms of an equivalent length and if a friction factor correlation of the form $f=p/Re^b$ is valid throughout the loop

$$g\rho_r \overline{\beta}_h \oint (h-h_r)dz = \frac{p\mu_l^b W^{2-b}}{2\rho_l}\left\{\sum_{i=1}^{N_s}\left(\frac{L_{eff}}{D^{1+b}A^{2-b}}\right)_i + \sum_{i=N_s+1}^{N_B}\left(\frac{\overline{\phi}_{LO}^2 L_{eff}}{D^{1+b}A^{2-b}}\right)_i + \phi_{LO}^2 \sum_{i=N_B+1}^{N_{tp}}\left(\frac{L_{eff}}{D^{1+b}A^{2-b}}\right)_i\right\}$$

It may be noted that the above assumption (i.e. $f=p/Re^b$) may not be valid always for reactor loops.

Steady state Performance of Two-phase Loops

$$g\rho_r \overline{\beta}_h \oint (h-h_r)dz = \frac{p\mu_l^b W^{2-b}}{2\rho_l}\left\{\sum_{i=1}^{N_s}\left(\frac{L_{eff}}{D^{1+b}A^{2-b}}\right)_i + \sum_{i=N_s+1}^{N_B}\left(\frac{\overline{\phi}_{LO}^2 L_{eff}}{D^{1+b}A^{2-b}}\right)_i + \phi_{LO}^2\sum_{i=N_B+1}^{N_{tp}}\left(\frac{L_{eff}}{D^{1+b}A^{2-b}}\right)_i\right\}$$

Nondimensionalizing the above with the following substitutions

$$\omega = \frac{W}{W_{ss}}; \mathcal{H} = \frac{h-h_r}{(\Delta h)_{ss}}; Z = \frac{z}{H}; S = \frac{s}{H}; a_i = \frac{A_i}{A_r}; d_i = \frac{D_i}{D_r}; l_i = \frac{L_i}{L_t} \; and \; (l_{eff})_i = \frac{(L_{eff})_i}{L_t}$$

$$where \; A_r = \frac{1}{L_t}\sum_{i=1}^{N_t} A_i L_i = \frac{V_t}{L_t}; D_r = \frac{1}{L_t}\sum_{i=1}^{N_t} D_i L_i; \rho_r = \rho_{in}; \; and \; h_r = h_{in}$$

$$\mathrm{Re}_{ss} = C\left(\frac{Gr_m}{N_G}\right)^r \qquad Where \; \mathrm{Re}_{ss} = \frac{D_r W_{ss}}{A_r \mu_l}; Gr_m = \frac{D_r^3 \rho_l^2 \beta_I g Q_h \mathrm{H}}{A_r \mu_l^3}; C = \left(\frac{2}{p}\right)^r \; and \; r = \frac{1}{3-b}$$

$$N_G = \frac{L_t}{D_r}\left\{\sum_{i=1}^{N_s}\left(\frac{l_{eff}}{d^{1+b}a^{2-b}}\right)_i + \overline{\phi}_{LO}^2\sum_{i=N_s+1}^{N_B}\left(\frac{l_{eff}}{d^{1+b}a^{2-b}}\right)_i + \phi_{LO}^2\sum_{i=N_B+1}^{N_{tp}}\left(\frac{l_{eff}}{d^{1+b}a^{2-b}}\right)_i\right\}$$

$$\mathrm{Re}_{ss} = 0.1768\left(\frac{Gr_m}{N_G}\right)^{\frac{1}{2}} \text{ laminar loop}$$

$$and \; \mathrm{Re}_{ss} = 1.96\left(\frac{Gr_m}{N_G}\right)^{\frac{4}{11}} \; turbulent \; loop$$

Special Cases

Single-phase natural circulation

$$\phi_{LO}^2 = 1,\ so\ that\quad N_G = \frac{L_t}{D_r}\sum_{i=1}^{N_t}\left(\frac{l_{eff}}{d^{1+b}a^{2-b}}\right)_i \quad and \quad \beta_h = \frac{1}{\mathrm{v}}\left(\frac{\partial \mathrm{v}}{\partial h}\right)_p = \frac{1}{\mathrm{v}}\left(\frac{\partial \mathrm{v}}{\partial (CpT)}\right)_p$$

$$If\ Cp\ is\ \text{constant, then}\ \beta_h = \frac{1}{\mathrm{Cpv}}\left(\frac{\partial \mathrm{v}}{\partial T}\right)_p = \frac{\beta_T}{Cp} \quad where\ \beta_T = \frac{1}{\mathrm{v}}\left(\frac{\partial \mathrm{v}}{\partial T}\right)_p\ so\ that\ we\ get$$

Single-phase NCL	Two-phase NCL
$W = \left[\frac{2\rho_r^2 \overline{\beta}_T g Q_h H}{RC_p}\right]^{\frac{1}{3}}$	$W = \left[\frac{2\rho_r^2 \overline{\beta}_h g Q_h H}{R}\right]^{\frac{1}{3}}$
$R = \sum_{i=1}^{N_t}\left(\frac{fL}{DA^2} + \frac{K_{sp}}{A^2}\right)_i$	$R = \sum_{i=1}^{N_s}\left(\frac{fL}{DA^2} + \frac{K_{sp}}{A^2}\right)_i + \sum_{i=N_s+1}^{N_B}\left(\frac{\overline{\phi}_{LO}^2 fL}{DA^2} + \frac{K_{tp}}{A^2}\right)_i + \phi_{LO}^2 \sum_{i=N_B+1}^{N_{tp}}\left(\frac{fL}{DA^2} + \frac{K_{tp}}{A^2}\right)_i$
$\mathrm{Re}_{ss} = C\left(\frac{Gr_m}{N_G}\right)^r$	$\mathrm{Re}_{ss} = C\left(\frac{Gr_m}{N_G}\right)^r$
$N_G = \frac{L_t}{D_r}\sum_{i=1}^{N_t}\left(\frac{l_{eff}}{d^{1+b}a^{2-b}}\right)_i$ $and\ Gr_m = \frac{D_r^3 \rho_l^2 \beta_T g Q_h \mathrm{H}}{A_r Cp \mu_l^3}$	$N_G = \frac{L_t}{D_r}\left\{\sum_{i=1}^{N_s}\left(\frac{l_{eff}}{d^{1+b}a^{2-b}}\right)_i + \overline{\phi}_{LO}^2 \sum_{i=N_s+1}^{N_B}\left(\frac{l_{eff}}{d^{1+b}a^{2-b}}\right)_i + \phi_{LO}^2 \sum_{i=N_B+1}^{N_{tp}}\left(\frac{l_{eff}}{d^{1+b}a^{2-b}}\right)_i\right\}$ $and\ Gr_m = \frac{D_r^3 \rho_l^2 \overline{\beta}_h g Q_h \mathrm{H}}{A_r \mu_l^3}$

Two-Phase Natural Circulation

Extensive database exists for the steady state performance of two-phase loops. However, complete geometric details are not always available

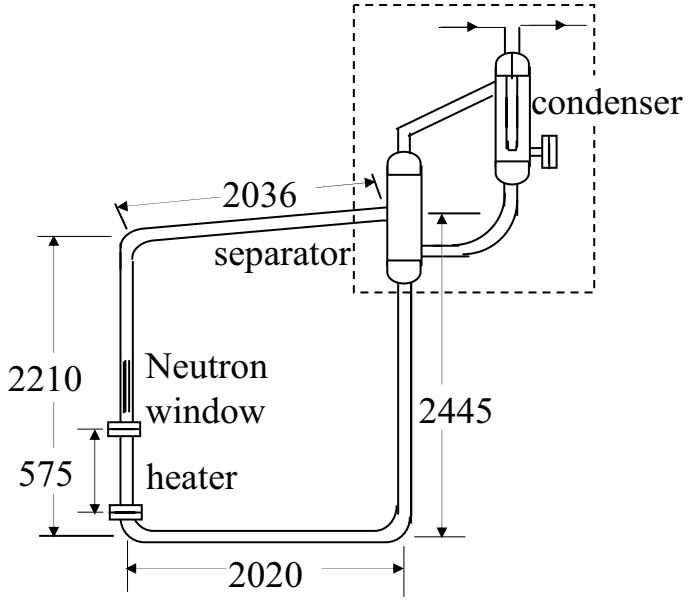

(a) 7, 9.1, 15.74 & 19.86 mm loops

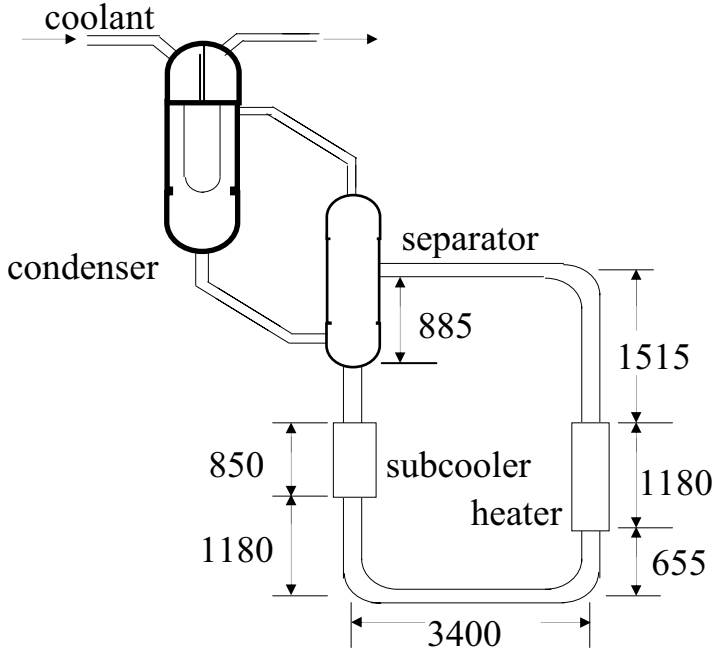

(b) 49.3 mm loop

Schematic of the different test loops

Range of Parameters of Data

Pressure : 0.1-7 MPa Power : 0.3-40 kW ΔT_{sub} : 0.1-16 K

Quality : 0.4-24% Diameter: 7, 9.1, 15.7, 19.9 & 49.3 mm

Steady state Performance of Two-phase Loops

Testing with correlation

Loops considered: 5

Literature data is not utilized as yet except one NDL data

The experimental data is in reasonable agreement with the theoretical correlation

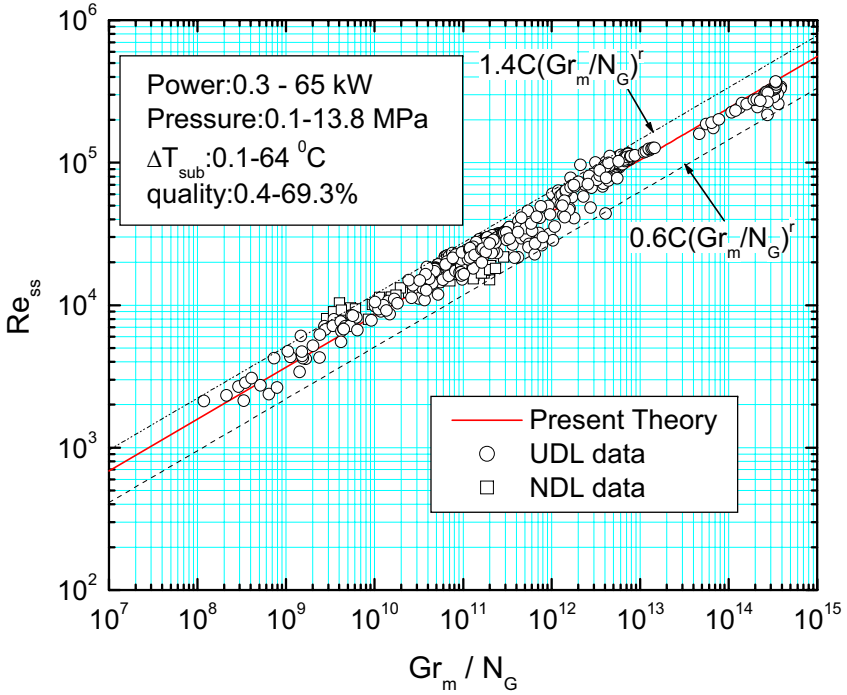

Testing of correlation with data

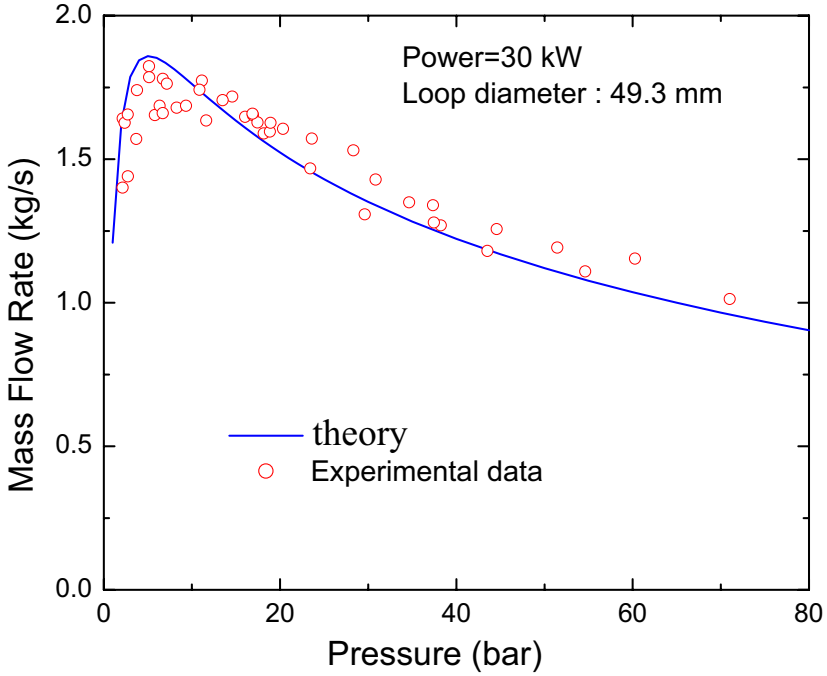

Effect of pressure on two-phase NC flow

At constant power, the flow rate goes through a peak and then reduces with increase in pressure

Effect of Power on Steady State Flow in 2-ϕ NCLs

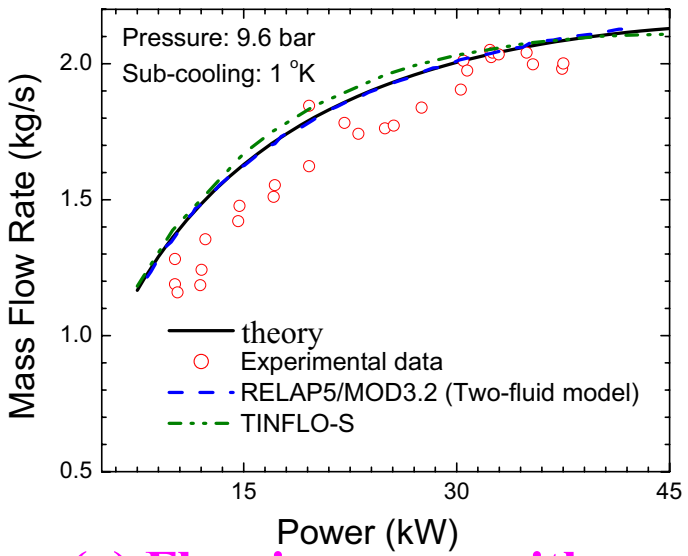

(a) Flow increases with power

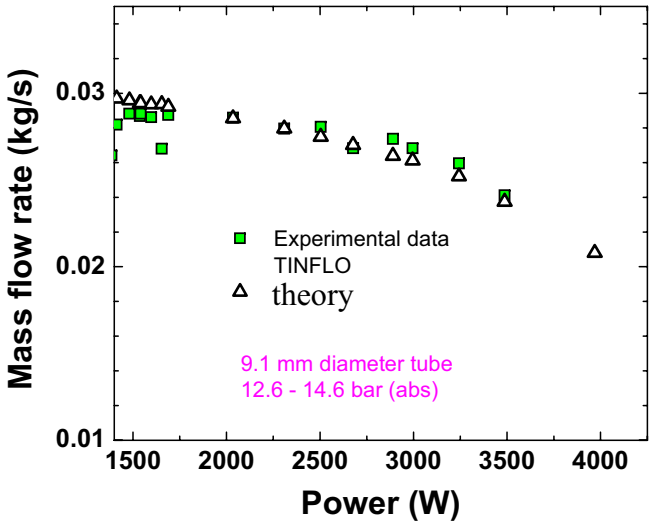

(b) Flow decreases with power

With increase in power, the steady state flow may increase, decrease or remain practically unaffected.

Different NC flow regimes exist in two-phase loops

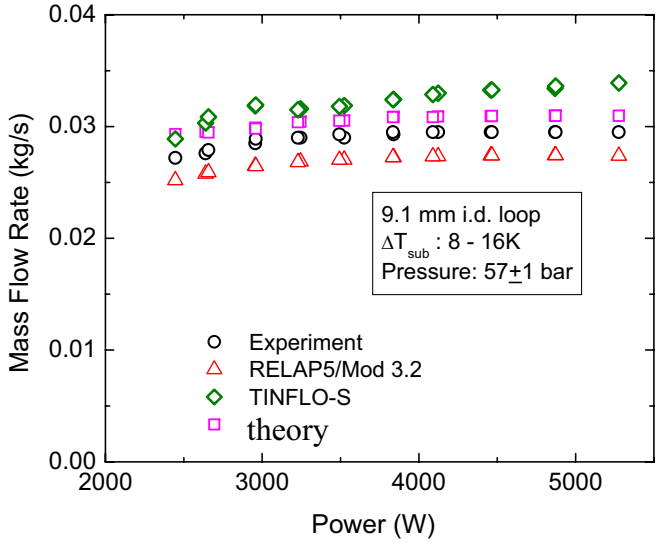

(c) Flow invariant with power

NC Flow Regimes in two-phase NCLs

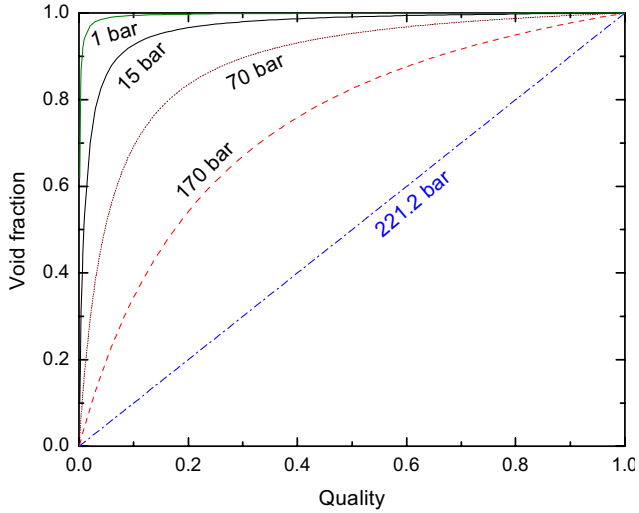

Effect of quality on void fraction

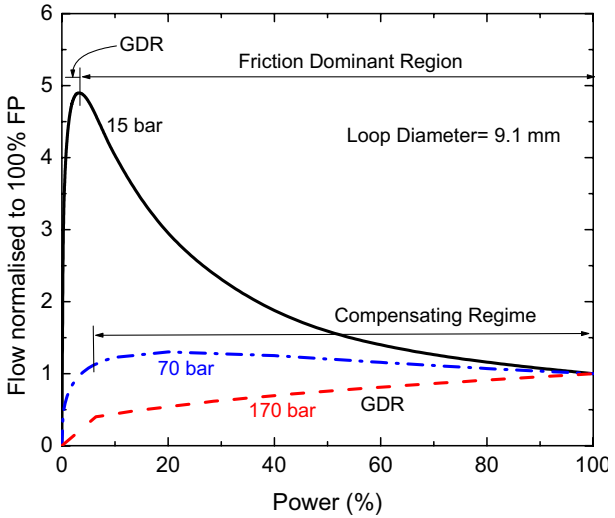

Different flow regimes in 9.1 mm loop

Gravity Dominant Regime: Occurs at low qualities where there is a large change in void fraction with small change in quality. Characteristic of this regime is that NC flow increases with power

Friction Dominant Regime: Occurs at high qualities where there is a small change in void fraction with change in quality. Characteristic of this regime is that flow decreases with increase in power. Generally observed during low power operation.

Compensating Regime: **The increase in buoyancy force is compensated by a corresponding increase in frictional force resulting in practically constant flow**

Effect of Loop Diameter on two-phase NC Flow Regimes

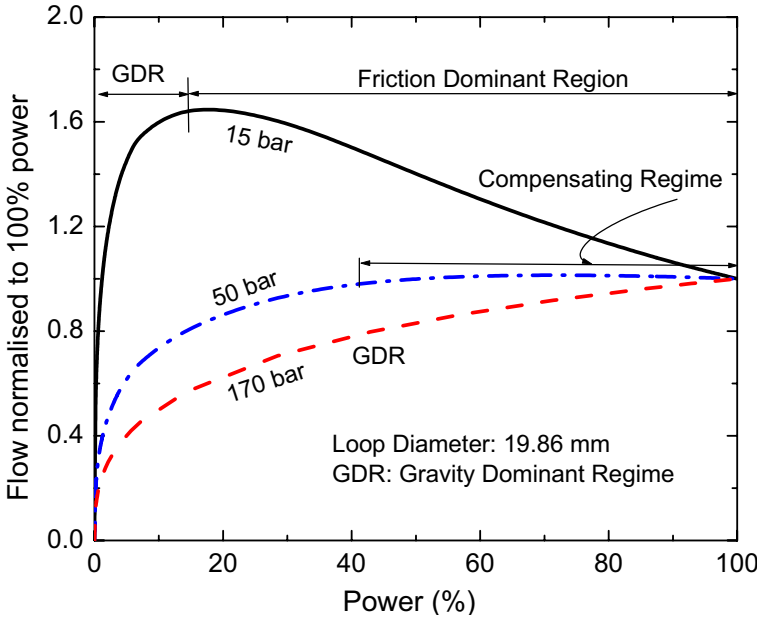

(a) 19.86 mm loop

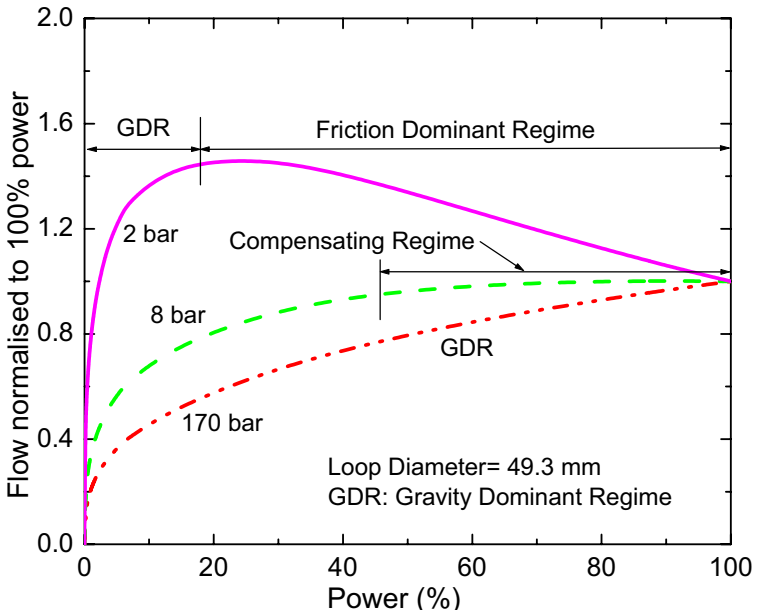

(b) 49.3 mm loop

The friction dominant regime shifts to lower pressures with increase in loop diameter

At high pressures, only the gravity dominant regime may be observed if the power is low.

Knowledge of the flow regimes helps to understand the stability behaviour of two-phase loops

Stability Behaviour of Single-phase Loops

Extensive database exists on single-phase instability and a few of the general characteristics observed are discussed below

- Hysteresis
- Instability mechanisms and flow regimes
- Flow regime switching and oscillation period
- Limit cycles
- Effect of power
- Prediction of instability threshold
- Prediction of limit cycles
- Techniques for stabilization

Hysteresis Phenomenon

From the linear analysis, it appears that the stability threshold is a unique value.

A region of hysteresis (conditional stability) exists where the instability threshold depends on the operating procedure

The phenomenon is observed in simple rectangular loops, figure-of-eight loops with throughflow, parallel channel systems and two-phase loops

The effect of the following three operating procedures are investigated

- Start-up from rest (Instability threshold: 105 W)
- Power raised from stable steady state (Threshold : 270 W)
- Power step back from an unstable state (Threshold : 60 W)

The instability thresholds were found to be different for all the three cases with the coolant secondary conditions maintained constant

Oscillatory flow regimes

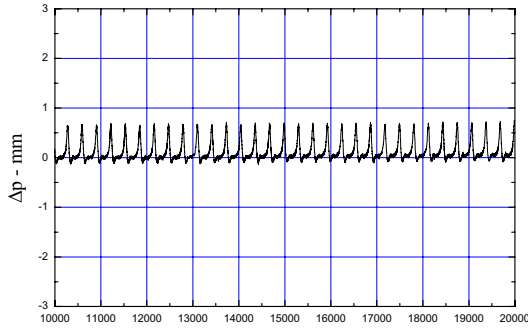

(a) time series for unidirectional pulsing

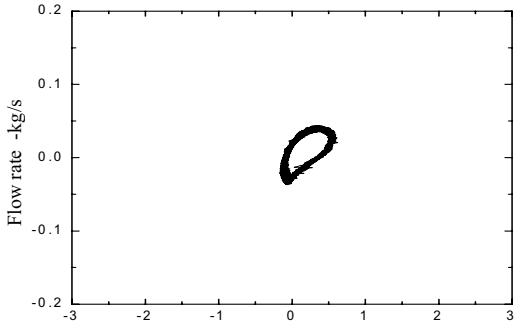

(b) limit cycle for unidirectional pulsing

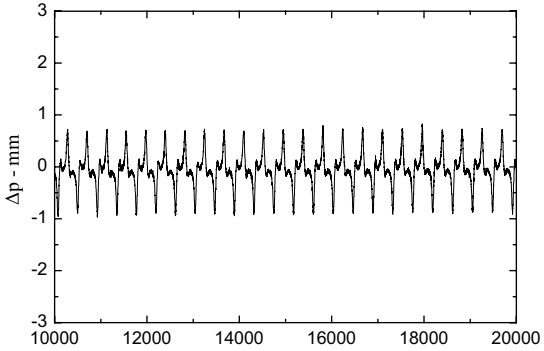

(c) time series for bi-directional pulsing

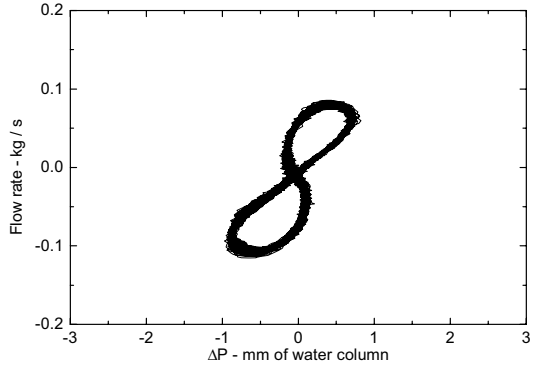

(d) limit cycle for bi-directional pulsing

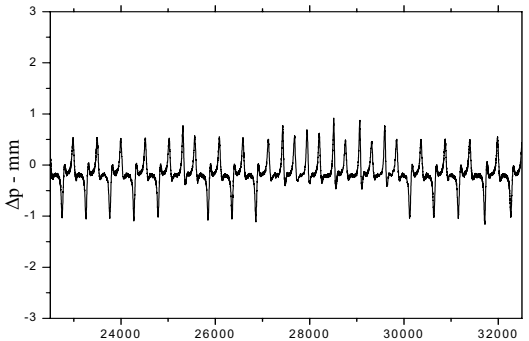

(e) time series for chaotic switching

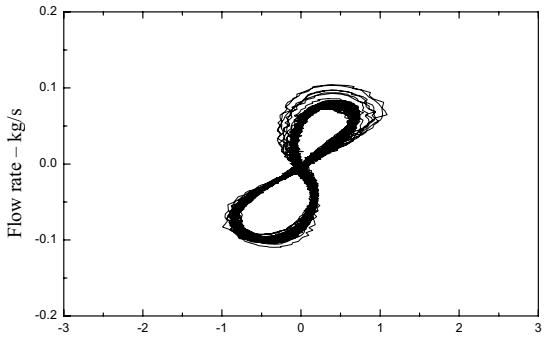

(f) limit cycle for chaotic switching

A rich variety of oscillatory flow regimes are possible
-unidirectional
-bi-directional
-chaotic switching

The shape of the limit cycle depends on the chosen parameter space

Mechanism causing instability

Welander proposed that oscillation growth as the mechanism causing instability

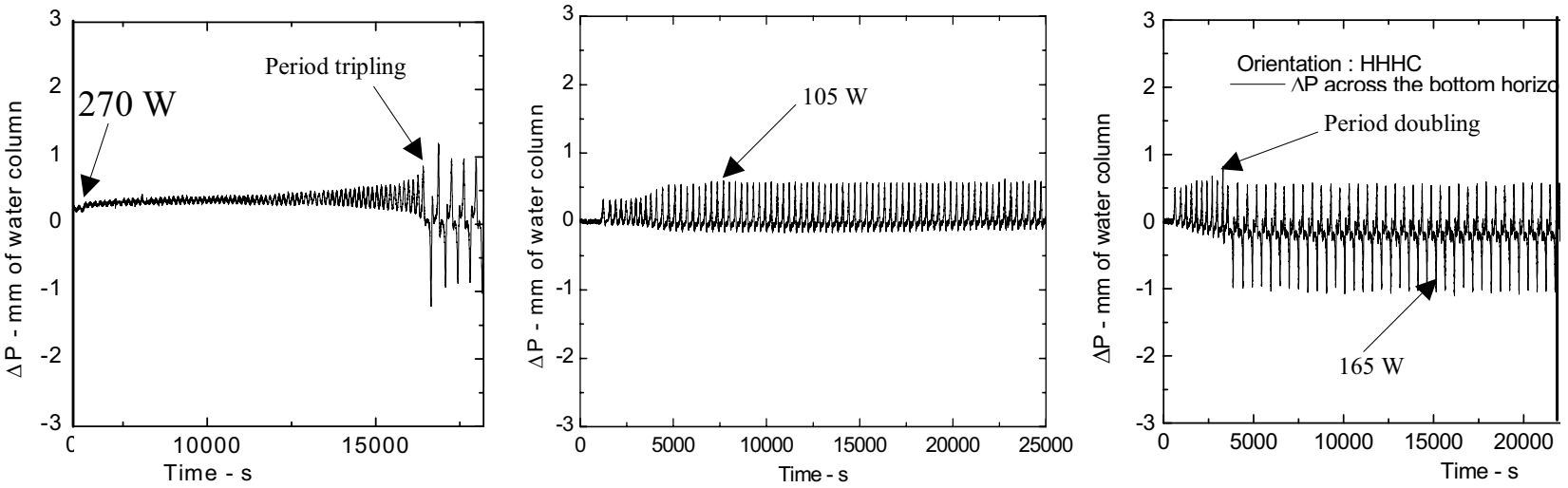

(a) Oscillation growth from steady state (b) Start-up from rest at low power c) Start-up from rest at high power

Oscillation growth is the mechanism causing instability. But differences are visible

Flow regime switching leads to period jump

Effect of power

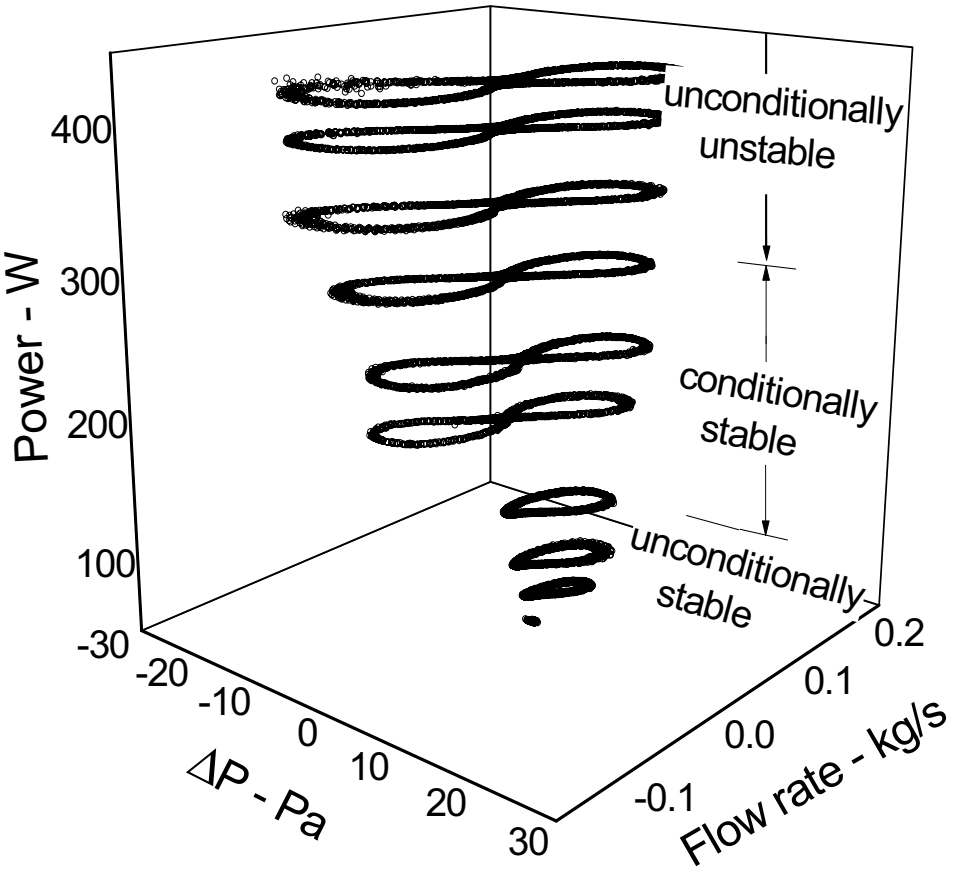

The amplitude of oscillation is found to increase with power.

The oscillations also become more chaotic with increase in power

The phase plots also deform with increase in power

Experimental 3-D Phase space of 1-Φ NC

The various flow regimes like unconditionally stable, conditionally stable (hysteresis) and the unconditionally unstable

Effect of power

The frequency of oscillation increases with increase in power except when period jump occurs

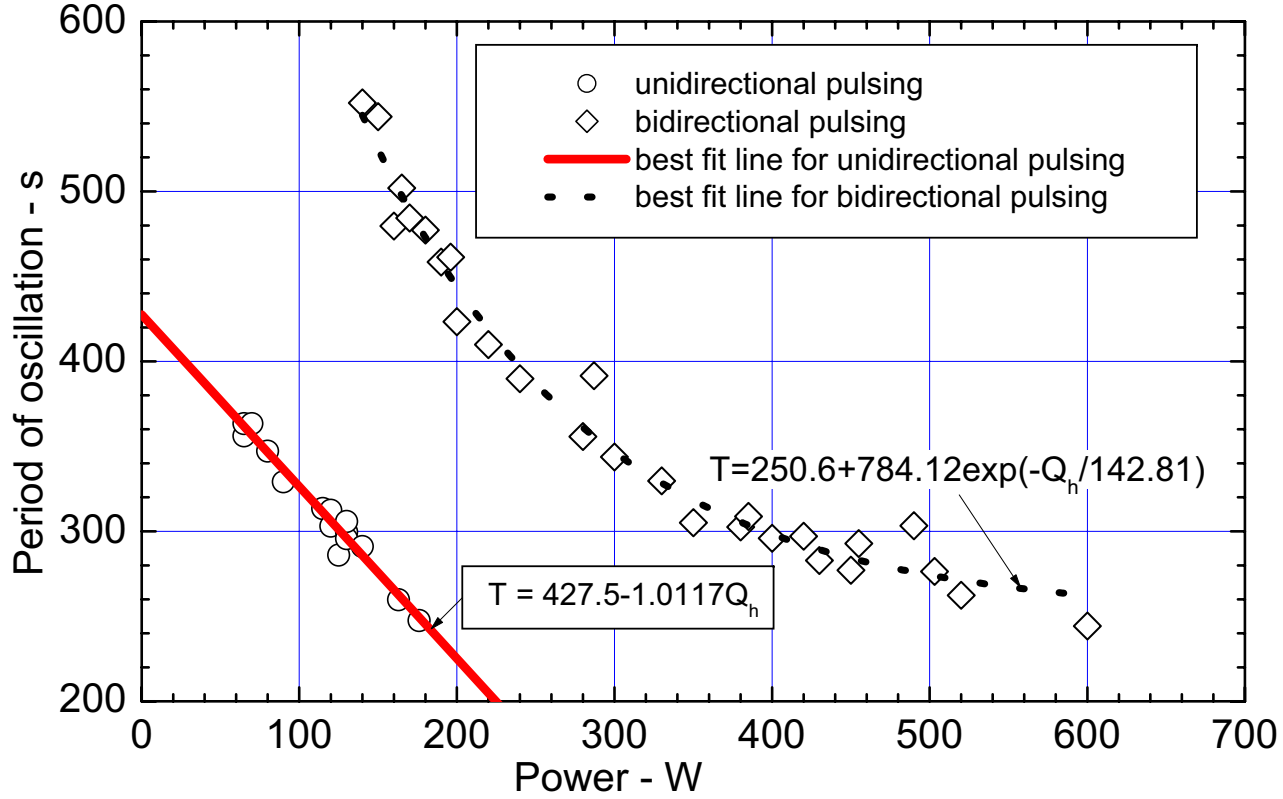

The period of unidirectional oscillation is found to decrease linearly where as the period of bi-directional oscillation is found to decrease exponentially

Prediction of Stability Map

The stability map is usually predicted by the linear theory

Often the wall effects and heat losses are neglected

The prediction is significantly affected by the friction factor correlation

Good comparison with experimental data is obtainable with a loop specific empirical correlation.

The same correlation when used for other loops can show significantly different results

However, accounting for the wall and heat loss effects good prediction can be expected for fully laminar and turbulent loops

For certain loop geometry such as the toroidal loop, the adequacy of 1-D theory is questionable due to the continuous variation of the gravitational component

Prediction of Limit Cycles

1-D theory is expected to give good prediction of the steady state flow if the local losses are accounted for a fully laminar and fully turbulent loop.

Good prediction of the stability map is also expected for the fully laminar and fully turbulent loop if wall thermal effects and heat losses are accounted

However, prediction of the limit cycle oscillations is a bigger challenge in single-phase loops as all three (laminar, turbulent and transition regimes) are encountered in rapid succession especially when periodic flow reversal takes place.

In such cases, a criterion for laminar to turbulent flow transition is also required. Different transition criteria also can give interesting results

The predicted limit cycles can be significantly different due to the 3-D effects caused by the flow which is never fully developed

Techniques for stabilizing

Increasing the St_m and L_t/D are always stabilizing.

Instability is observed in loops with $L_t/D < 300$.

Increasing the L_t/D is commonly used in NCSs. Introduction of orifices is the usual method. The location of the orifice does not matter in single-phase systems

Introduction of orifices reduce the flow and heat transfer capability significantly.

There are techniques which does not affect the flow

Use of thick conducting walls are found to stabilize single-phase systems

In addition process control techniques are being tried out to stabilize single-phase NCSs

Database for instability of two-phase NC loops

Extensive database from simple loop facilities exist for two-phase NC instability

Most instabilities such as flashing, geysering, Type I DWI, Ledinegg type instability and even CHF induced instability are found to occur during initiation of boiling.

For analysis purposes, it is important to separate them out based on their mechanism and characteristics as analysis methods are different

This is often lacking in the database

Experimental Stability Map (2-ϕ NC)

Two unstable regions are found for two-phase NCLs.

The first unstable zone in the two-phase region occurs at a low power and hence at low quality and is named as type I instability by Fukuda and Kobori (1979). Similarly, the second unstable zone in the two-phase region occurs at high powers and hence at high qualities and is named as type II instability.

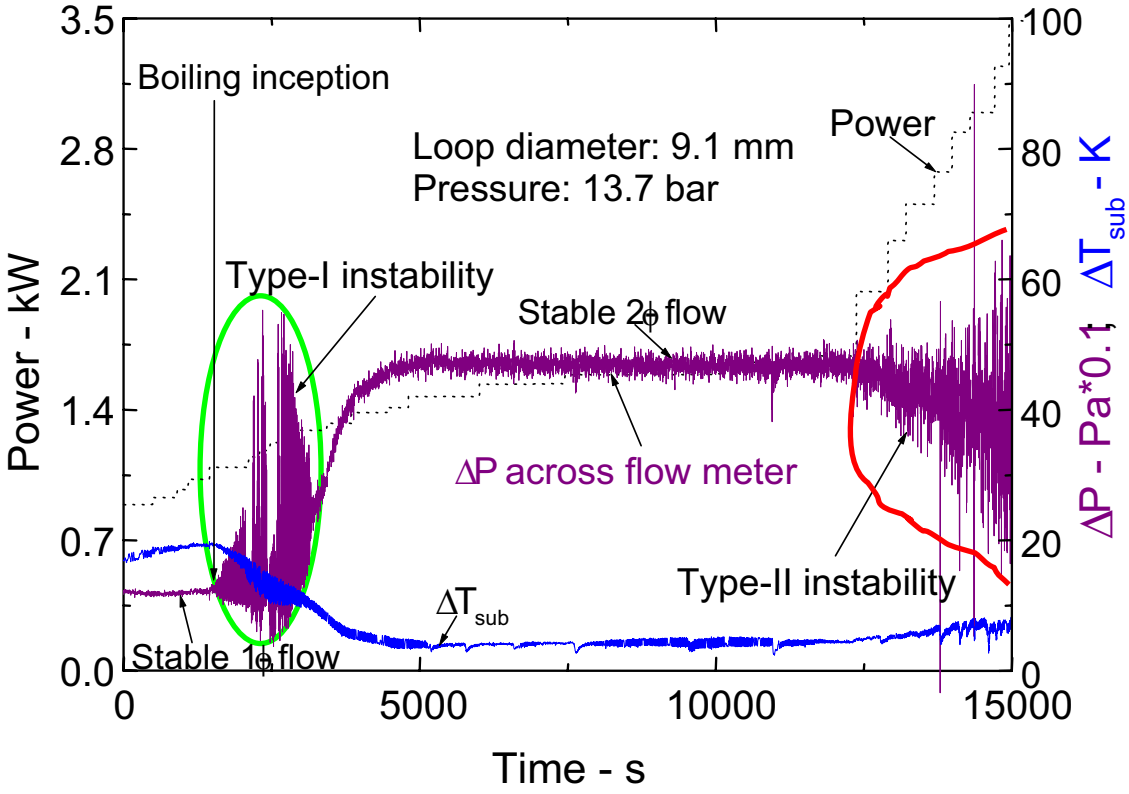

Typical low power and high power instability

Type-I instability occurs in the gravity dominant regime whereas type-II instability occurs in the friction dominant regime. Instability is not found in the compensating regime during the present tests.

Experimental Findings on Type-I Instability

It occurs right from the boiling inception. The amplitude of oscillations first increases, reaches a peak and then decreases with increase in power eventually leading to stable flow.

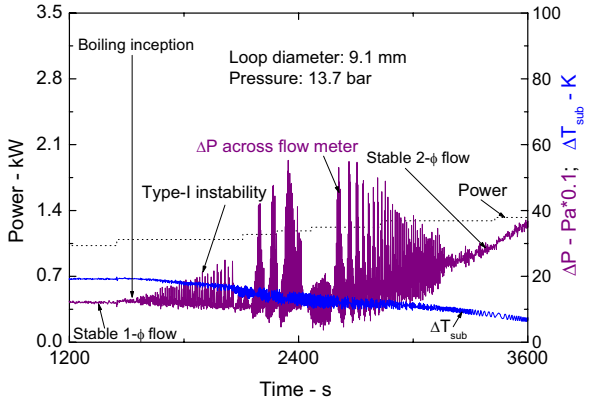

Generally unidirectional oscillations, but more chaotic than single-phase NC

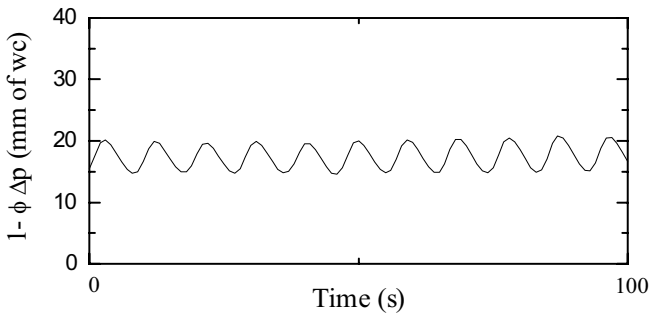

(a) Power = 20 kW

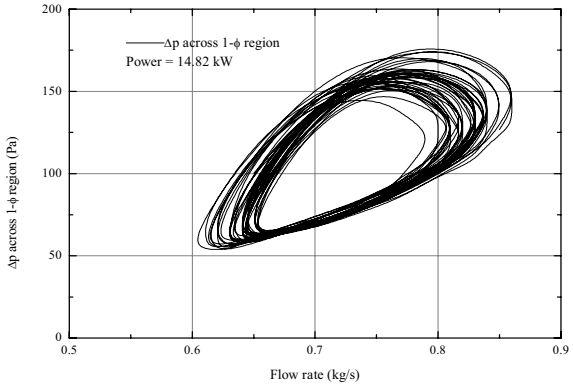

Phase plot at 15 kW and 2.2 bar

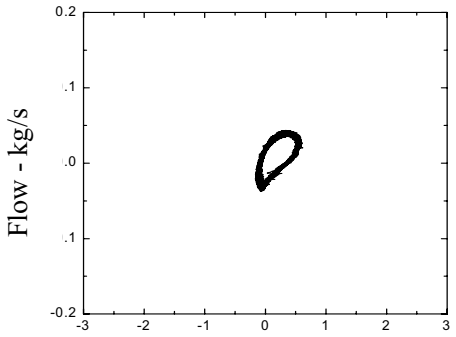

Limit cycle for UDO in single-phase loop

The limit cycle is similar to that found in single-phase flow except that it is more chaotic. Very few studies on validation of limit cycles

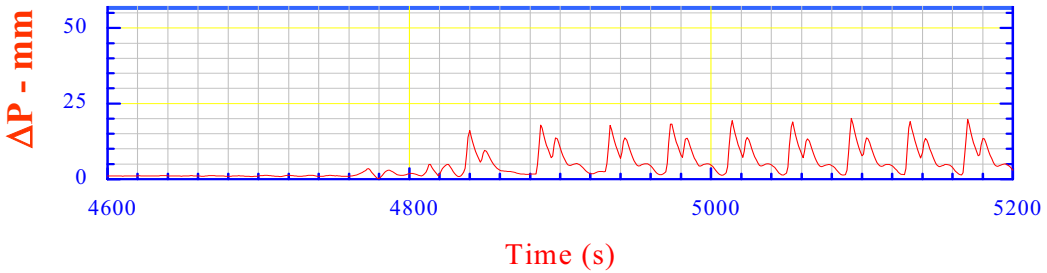

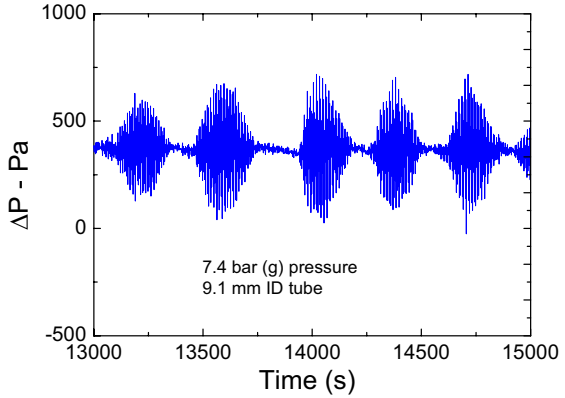

Experimental Findings on Type-I Instability

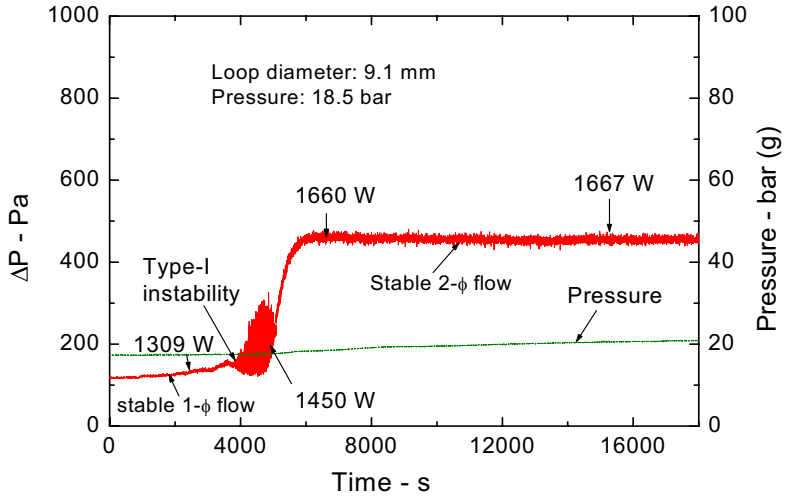

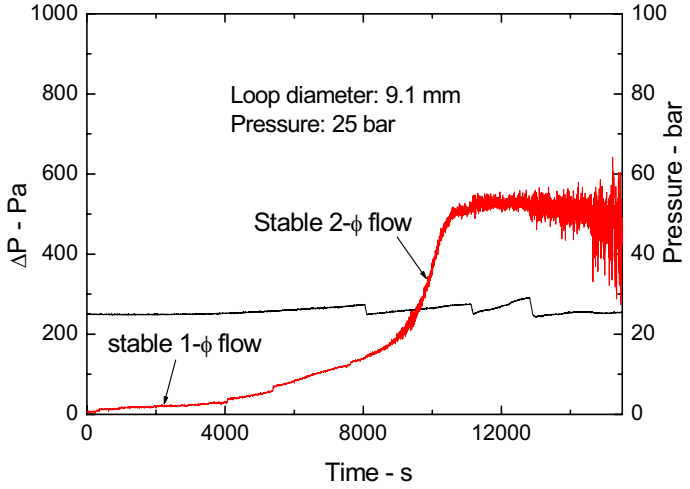

The amplitude of type-I oscillations reduce significantly with increase in pressure. Further, type-I instability is not observed beyond a critical value of the system pressure.

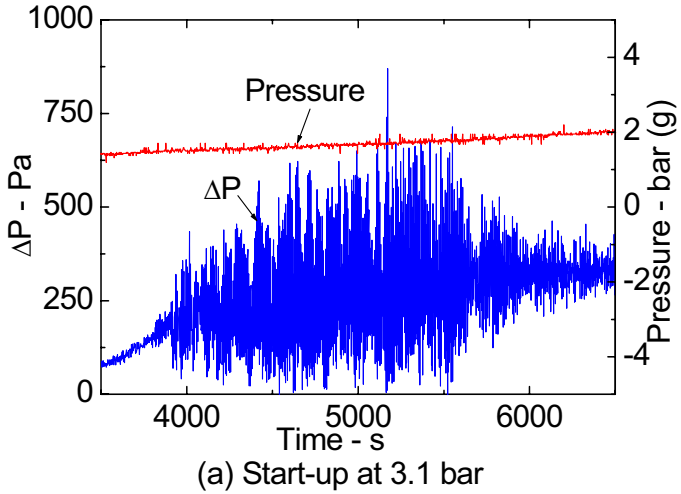

(a) Start-up at 3.1 bar

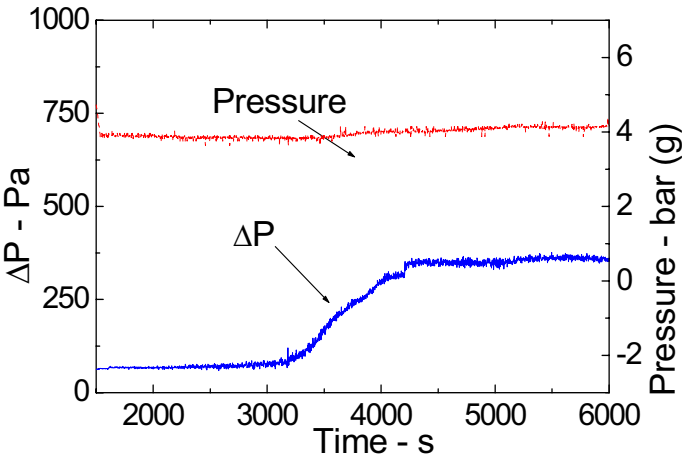

(b) Start-up at 5.4 bar

The critical value of pressure beyond which type-I instability disappears is found to decrease with increase in the loop diameter.

Effect of pressure on the instability due to boiling inception in 19.2 mm i.d. loop

Experimental Findings on Type-II Instability (2-ϕ NC)

Type-II instability is found to occur after the flow starts to decrease with increase in power in the present experiments. Type-II instability occurs in the friction dominant regime and it occurs at higher qualities.

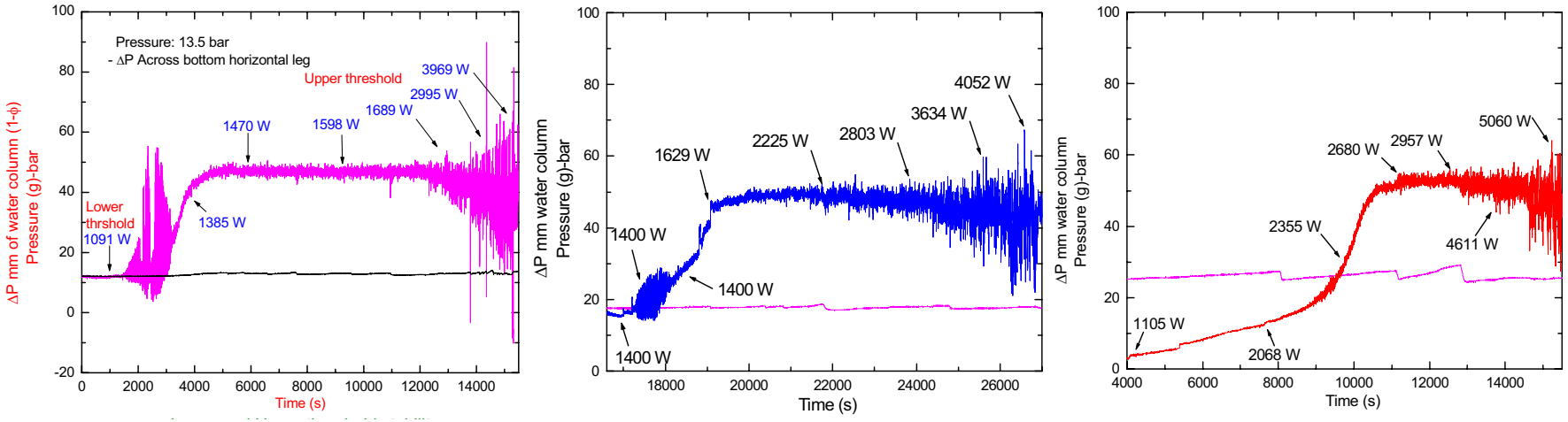

(a) 13 bar (b) 18 bar (c) 25 bar

The upper threshold of instability at different pressures

A general characteristic of the type-II instability is that the oscillation amplitude keeps increasing with power.

Prediction of Stability Map

Linear analysis based on the drift flux model is given by Ishii-Zuber (1970)

Saha and Zuber (1978) modified this model by taking into account the effect of thermal nonequilibrium effect.

Thermal nonequilibrium effect predicts a more stable system at low subcooling compared to thermal equilibrium model

These predictions showed poor agreement at high subcooling conditions when compared to experiments

Furutera (1986) showed that the threshold of instability could be predicted with reasonable accuracy using the homogeneous model. However, the two-phase friction multiplier and the heat capacity in the subcooled boiling region has a significant effect

Since then many others showed that it is possible to predict the threshold of DWI using HEM

Theoretical Findings on Instability (2-ϕ NC)

The stability of the test loops were studied with a linear stability code TINFLO-S based on the drift flux model. The drift flux parameters (Co and Vgj) for slug flow were used as it was the most frequently observed flow pattern during the tests. The Martinelli-Nelson two-phase friction multiplier model was used in the computations.

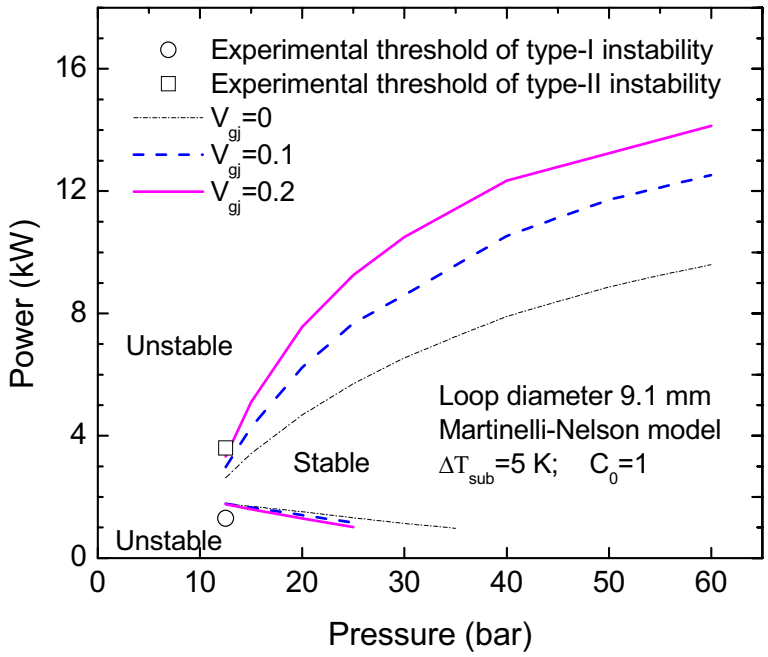

(a) Effect of drift velocity

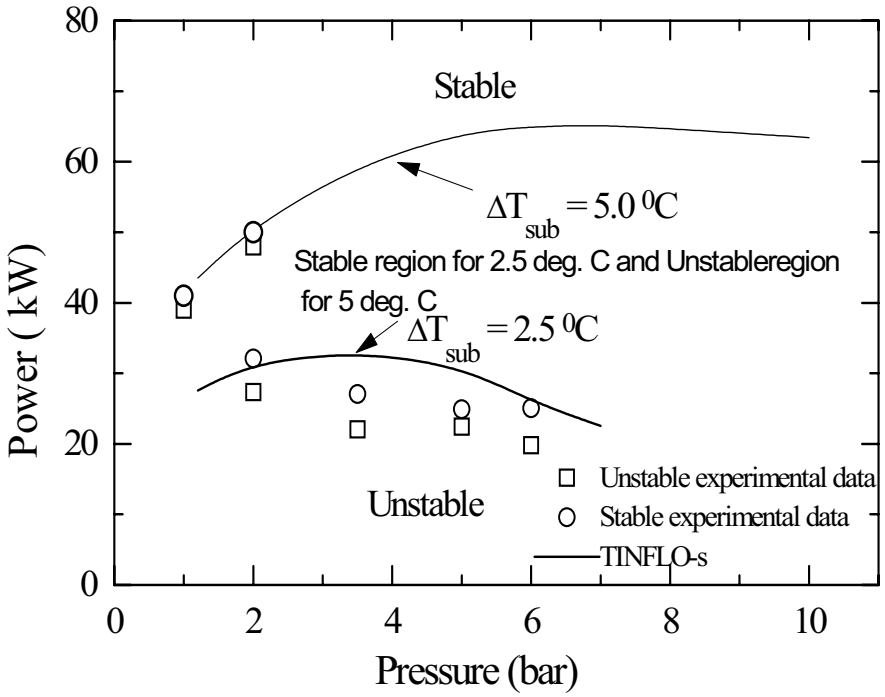

(b) Effect of subcooling

Comparison of measured and predicted stability maps

Theoretical Findings on Instability (2-ϕ NC)

Effect of loop diameter on stability

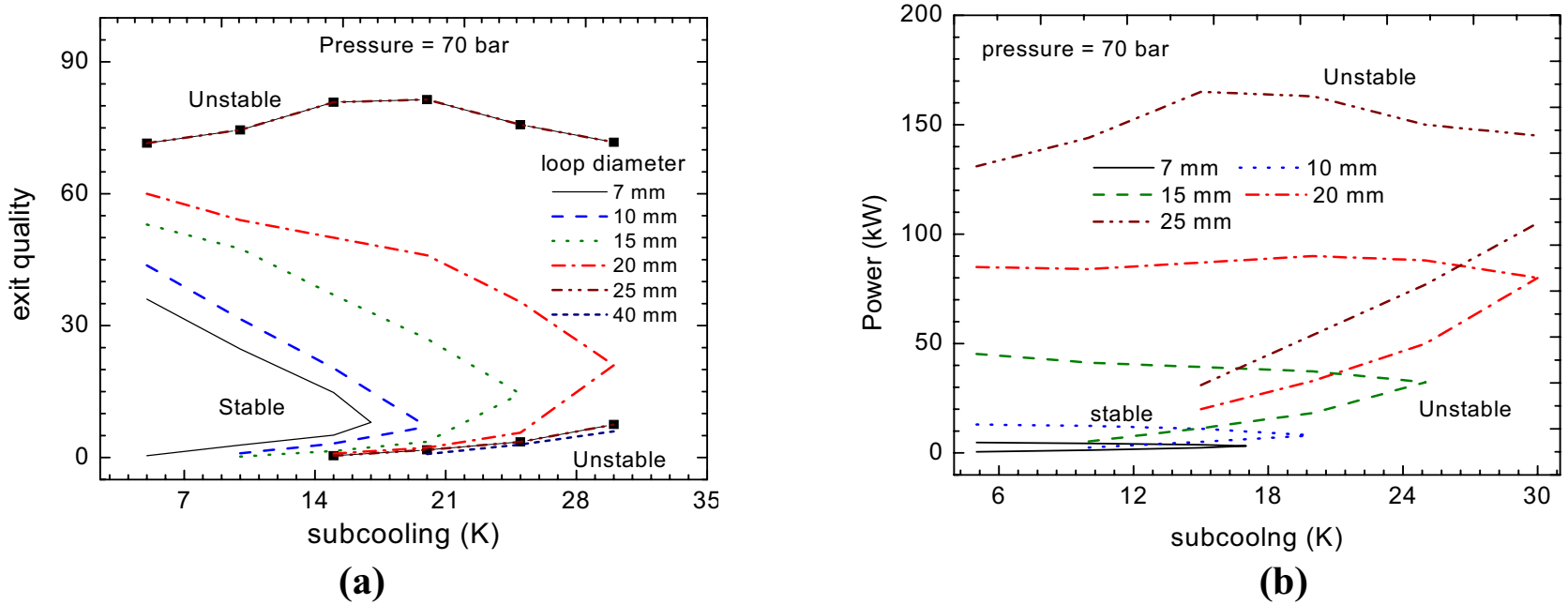

(a) **(b)**

Predicted stability map for various loop diameters

The stable zone enhances with increase in loop diameter which is consistent with the test results.

Type-II instability threshold shifts to higher qualities with increase in loop diameter. Beyond 40 mm loop diameter, the upper threshold is not found in the two-phase region (i.e. 0<quality≤1).

Design Considerations (2-ϕ NC)

By appropriate choice of the loop diameter, it is possible to eliminate the type-II instability in the two-phase loops.

Since both instability and CHF needs to be avoided in the design of two-phase natural circulation systems two types of designs are possible depending on which of them is limiting the maximum power that can be extracted.

Stability-Controlled Designs

The maximum power is limited by the stability, as the threshold of type-II instability is lower than the CHF threshold. This situation arises in small diameter loops.

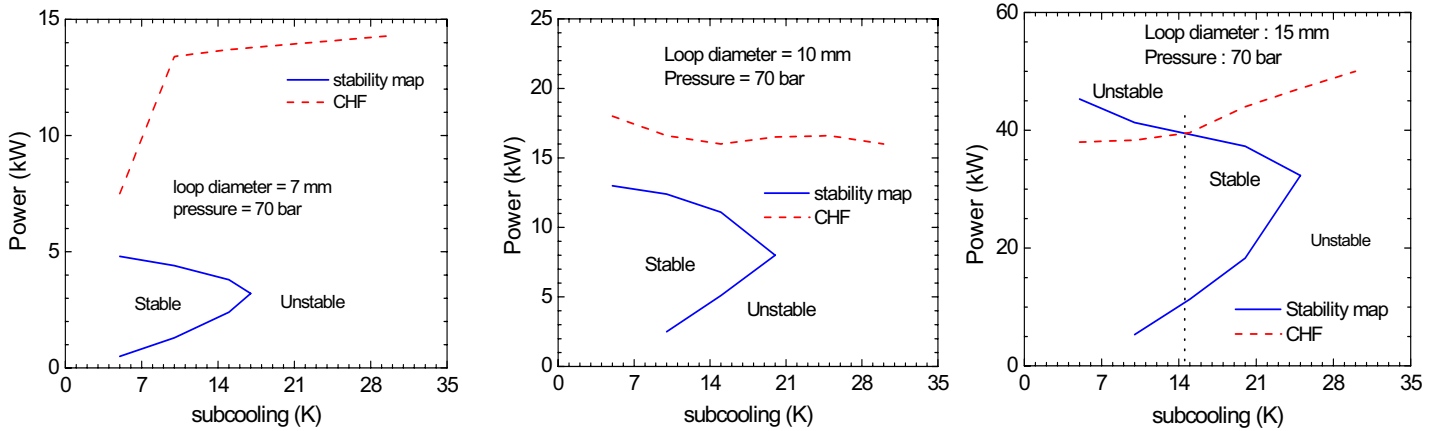

(a) 7mm loop **(b) 10mm loop** **(c) 15 mm loop**

Stability controlled designs and loop diameter

Design Considerations (2-ϕ NC)

CHF-controlled Designs

The CHF threshold is much below the type-II instability threshold and hence CHF limits the maximum power that can be extracted. This situation arises in large diameter loops.

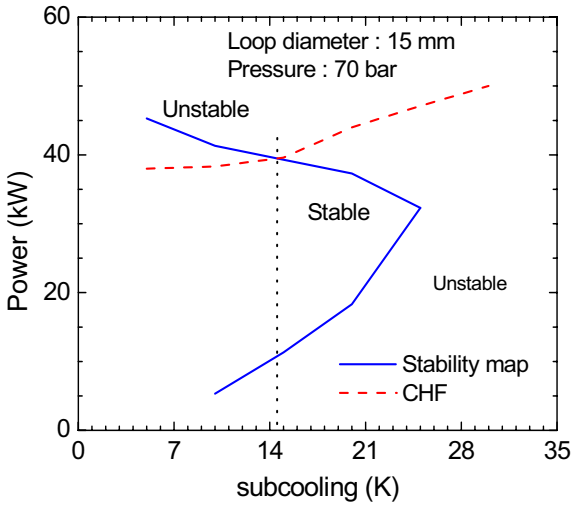

(a) 15 mm

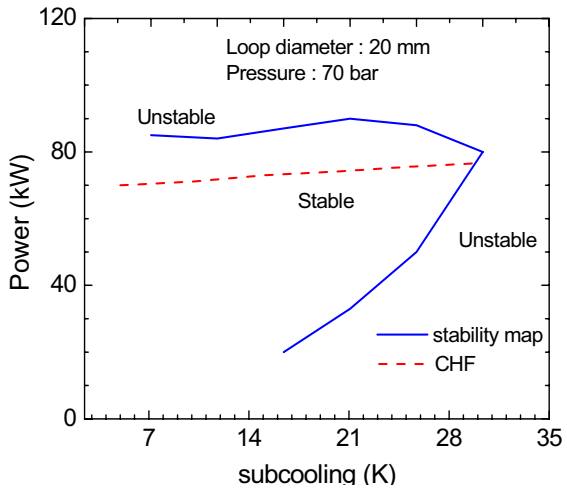

(b) 20 mm loop

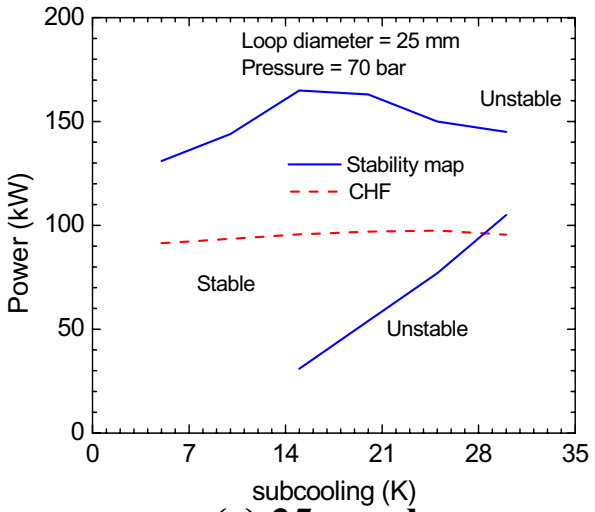

(c) 25 mm loop

CHF controlled designs and effect of loop diameter

Design of forced circulation BWRs is usually CHF controlled.

Design Considerations (2-ϕ NC)

Operating line for stability controlled designs

Since two-phase NCSs are not completely stable over the entire subcooling-power map an operating line needs to be specified for ensuring stability for all anticipated operations like start-up, power raising, and step back. The decay ratio goes through a minimum while moving from the lower to the upper threshold for a fixed subcooling. Ideally, the operating line shall pass through the minimum decay ratio line (locus of all minimum decay ratio points) so that all oscillations will die down in the quickest possible manner.

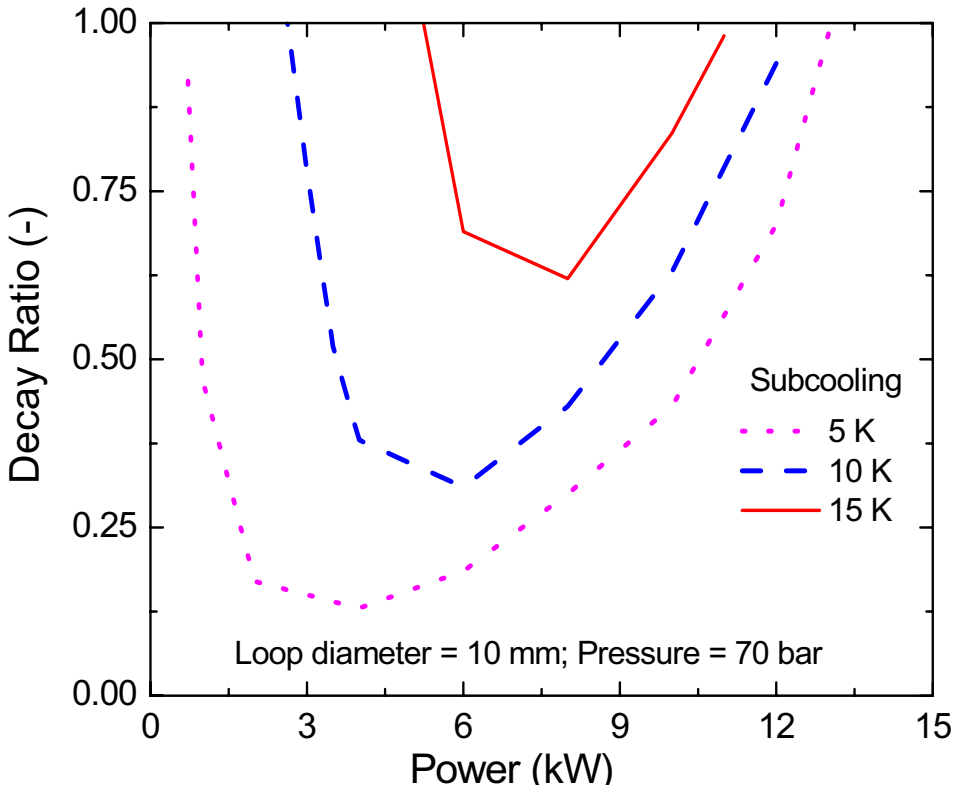

Variation of decay ratio while going from the lower to the upper threshold

For stability-controlled designs, one could choose the operating line as the minimum decay ratio line

Design Considerations

Unstable oscillations and CHF

Premature occurrence of CHF and test section burnout can be an issue during oscillatory flows in two-phase loops. In the present experiments, premature CHF occurrence was observed only for the test section diameters of 7 and 9.1 mm. The occurrence of burnout during instability was more frequent in 7 mm diameter loop than in 9.1 mm loop. Inspection of the burnt out test sections revealed that the burnout is not restricted to the test section outlet.

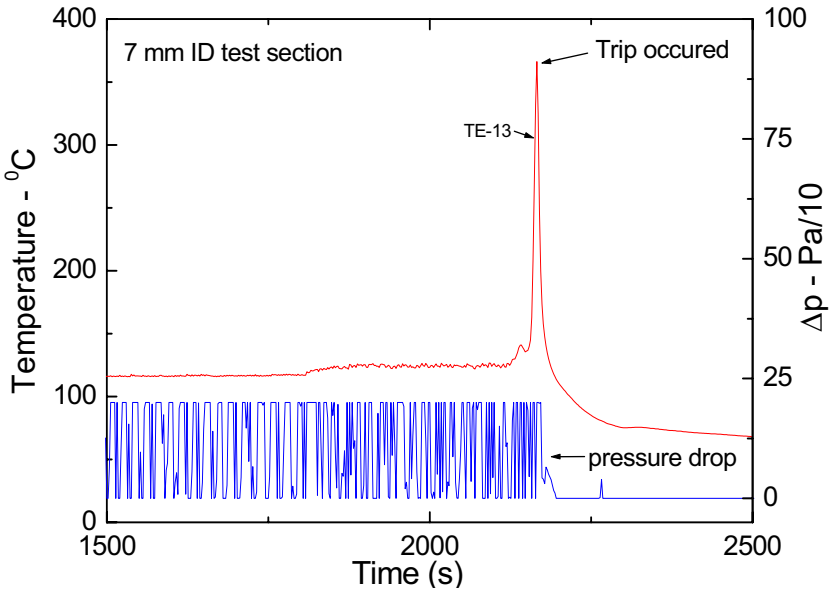

Typical CHF occurrence during oscillatory flow

In the larger diameter test sections, the CHF power was significantly large compared to the available power preventing the burnout during unstable oscillatory flow.

Premature Occurrence of CHF

Premature occurrence of CHF is a problem at low oscillation frequency. It is also important at high frequencies if the oscillation amplitude is large

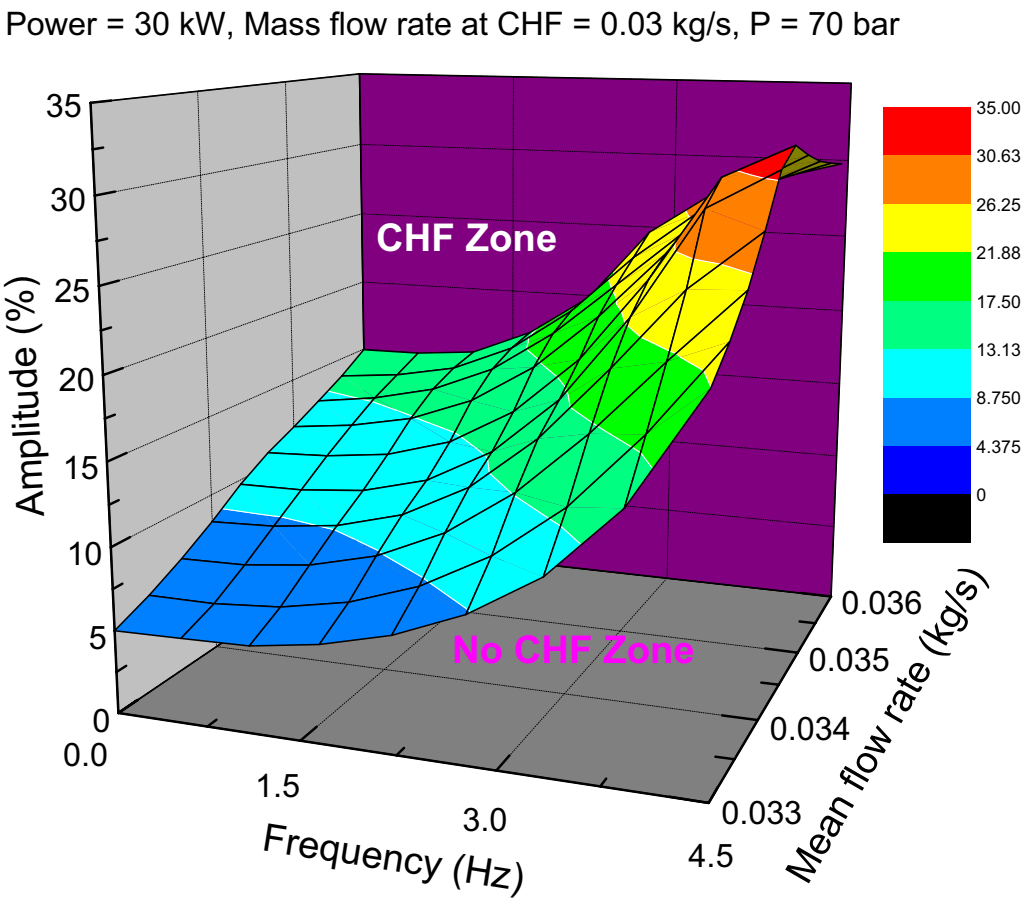

Concluding Remarks

Single-phase Loops

Using a generalized dimensionless relationship, it is possible to compare the steady state performance of different loops

Friction factor correlations, wall thermal capacitance and heat losses significantly affect the prediction of instability threshold

Reasonable prediction of the threshold is possible for fully laminar and fully turbulent loops if the wall thermal capacitance and heat losses are accounted

1-D theory is able to predict the trend of the time series and the different unstable flow regimes. However, the shape of the limit cycles are significantly different.

3-D effects are important for unstable oscillatory flows and the applicability of 1-D theory for the prediction of limit cycles is debateable

Concluding Remarks

Two-phase loops

Lack of generalized dimensionless groups make it difficult to compare the steady state performance of different loops

Although, extensive database exists, often it is not possible to identify the instability type from the data

The threshold of instability can be predicted with reasonable accuracy using the homogeneous model. However, the two-phase friction multiplier and the heat capacity in the subcooled boiling region has a significant effect

Very few studies are reported for the validation of the observed limit cycles

Thank you